13

TMD factorization

An appealing interpretation of a parton density is that it is a number density of partons in a target hadron. As we saw in Sec. 6.7, a parton density in a simple theory is an expectation value of a light-front number operator, integrated over transverse momentum. A similar interpretation applies to fragmentation functions: Sec. 12.4.

As explained in Secs. 6.8 and 12.4, it is equally natural to define unintegrated, or transverse-momentum-dependent (TMD), parton densities and fragmentation functions, simply by omitting the integral over transverse momentum. In a sense, the TMD functions are more fundamental and present more information on non-perturbative phenomena than do the ordinary integrated functions. Therefore it is useful to find situations where TMD functions are needed.

In this chapter, I treat two characteristic cases. One is two-particle-inclusive e^+e^- annihilation when the detected hadrons are close to back-to-back. This process needs TMD fragmentation functions. Then I will extend this work to semi-inclusive DIS (SIDIS) with a detected hadron of low transverse momentum. In SIDIS, TMD parton densities are needed as well as fragmentation functions. A further extension to the Drell-Yan process at low transverse momentum will be covered in Sec. 14.5.

There are substantial complications in QCD. Although the discussion about light-front quantization and the associated definitions of number densities gives a general motivation, it does not work correctly in QCD (or any other gauge theory). The actual definitions are whatever is appropriate to consistently obtain a valid factorization theorem.

The generally used jargon is that factorization with integrated pdfs and fragmentation functions is called "collinear factorization", while factorization with the unintegrated functions is called "k_T factorization". For the second case, I prefer "TMD factorization". Its overall structure generalizes the results for the Sudakov form factor in Ch. 10.

13.1 Overview of two-particle-inclusive e^+e^- annihilation

The definition of an ordinary integrated pdf or fragmentation function arises from the approximants used in deriving factorization. There are two parts to an approximant. One is in the actual amplitude for the hard scattering, where we neglect transverse and
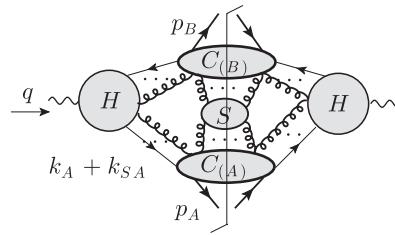
479

Fig. 13.1. A leading region in gauge theory for two-hadron-inclusive cross section in e^+e^- annihilation. Like Fig. 12.4(a), but with an extra detected hadron.

minus components of momentum with respect to Q. The other is in the kinematics of some groups of the final-state particles, as when some components of a jet or soft momentum are neglected relative to the large component of momentum in some other jet subgraph.

It is the second part of the approximant that determines the definition of a pdf or fragmentation function, and it can fail, even when the more fundamental first part of the approximant remains valid. Consider, for example, the collinear momentum k_A entering one jet subgraph in Fig. 12.4(a) or Fig. 12.5(a), and complete the loop by circulating it through the other jet subgraph. Neglecting k_A^- and $\boldsymbol{k}_{A\,\mathrm{T}}$ in the second jet amounts to changing the kinematics of the jet. If the jet is not observed, this gives a legitimate approximation for the inclusive cross section, as we showed more formally by routing the momentum out through the virtual photon, and by applying the approximant to the external test function in (12.11).

But the situation is quite different if, instead, we consider two-particle-inclusive annihilation $e^+e^- \to H_A H_B + X$ and choose the measured hadrons to be close to back-to-back. The leading regions are shown in Fig. 13.1, and a corresponding 2-jet final state was sketched in Fig. 12.19. Neglecting k_A^- in the second jet is still legitimate, because k_A^- is small and is neglected with respect to a large minus momentum in the unobserved part of the second jet.

But the neglect of $\boldsymbol{k}_{A\,\mathrm{T}}$ in the second jet is no longer justified. The neglect shifts the second detected hadron transversely by an amount that can be comparable (or even larger) than its transverse momentum relative to the jet. Exactly similar considerations apply to the approximant for the soft factor.

Therefore, a valid approximant must preserve the exact values of collinear and soft transverse momenta when they flow through other collinear subgraphs. A similar idea applies if we use a cross section averaged with a test function. Then we route loop integrals over soft and collinear subgraphs out through the photon vertex, and the approximant must preserve transverse momenta in the test function, unlike the definition in Sec. 12.8.1.

One direct consequence is that the relevant fragmentation functions are TMD functions, rather than the integrated functions. Another consequence is that the soft factor no longer

cancels. In one-particle-inclusive annihilation, we defined the soft factor with an independent integral over all momenta for its final state, thereby enabling the proof of cancellation in Sec. 12.8.6. But this fails when the transverse-momentum integral is coupled to the other factors. Our treatment must include the uncanceled soft factor, just as for the Sudakov form factor.

One simplification does occur, and this is that the leading regions in the back-to-back case only have two collinear subgraphs, as in Fig. 13.1. To understand this consider a region like Fig. 12.4(b), with three or more collinear groups, and for which a 3-jet final state was sketched in Fig. 12.18. We have two detected hadrons which are almost back-to-back, and so the directions of their parent jets are also almost back-to-back. Now, the propagators in the hard subgraphs are power-counted as having denominators of order Q^2. But as the directions of collinear subgraphs approach each other to give a 2-jet configuration, some denominators get much smaller, to approach collinear singularities. The neighborhood of these singularities therefore dominates the cross section. In the contribution to the cross section from a region with 3 (or more) collinear subgraphs, the 2-jet region is of course subtracted out, thereby giving a power-suppression relative to the 2-jet regions. Therefore, as claimed, the leading regions are restricted to those of Fig. 13.1, when the detected hadrons are close to back-to-back.

Deviations from the exact back-to-back configuration of the hadrons are controlled by transverse momentum within the two collinear subgraphs (and in the soft subgraph). Thus they are controlled by transverse momentum generated in fragmentation functions. This suggests a general pattern: TMD functions are needed whenever the directions of detected hadrons match a parton configuration that does not allow for extra jets.

13.2 Kinematics, coordinate frames, and structure functions

Much of the derivation uses the same elements that we already used in Ch. 12 and in earlier chapters. We focus on the changes.

In this section, we specify the kinematics and then define a hadronic tensor $W^{\mu\nu}$ for our process, together with corresponding structure functions. Let p_A and p_B be the momenta of the detected hadrons in $e^+e^- \to H_A H_B + X$, and let q be the momentum of the virtual photon. It is convenient to use two different coordinate frames:

- A *photon frame*, in which the photon has zero transverse momentum. This is chosen as a center-of-mass (CM) frame, supplemented by a condition on the direction of the z axis. It is a frame most directly related to an actual experiment, and is best suited for the analysis of the hard scattering.
- A *hadron frame*, in which the hadrons are back-to-back in the $\pm z$ directions. This matches the hadron frame used in (12.37) and (12.38) for defining fragmentation functions in momentum space.

Subscripts γ and h denote components of a vector in the two frames.
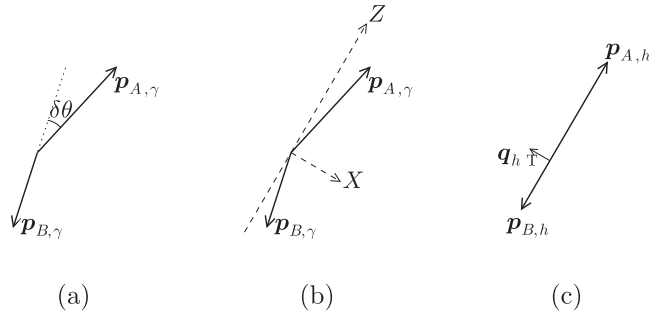
Fig. 13.2. Kinematics of two hadrons in final state: (a) center-of-mass frame; (b) center-of-mass frame with dashed lines to indicate Z and X axes used to define the structure functions in (13.9); (c) hadron frame of (13.4). *The incoming leptons in (a) and (b) can be out of the plane defined by the hadrons.*

13.2.1 Photon frame

Our standard photon frame, illustrated in Fig. 13.2(a), is a CM frame, where the momenta in ordinary Cartesian coordinates are

$$q_\gamma = (Q, \mathbf{0}), \tag{13.1a}$$

$$p_{A,\gamma} = \left(E_{A,\gamma}, \mathbf{p}_{A,\gamma}\right) \simeq |\mathbf{p}_{A,\gamma}| \left(1, \mathbf{n}_{A,\gamma}\right), \tag{13.1b}$$

$$p_{B,\gamma} = \left(E_{B,\gamma}, \mathbf{p}_{B,\gamma}\right) \simeq |\mathbf{p}_{B,\gamma}| \left(1, \mathbf{n}_{B,\gamma}\right). \tag{13.1c}$$

Here $\mathbf{n}_{A,\gamma}$ and $\mathbf{n}_{B,\gamma}$ are unit vectors for the directions of the hadrons. In the second form for $p_{A,\gamma}$ and $p_{B,\gamma}$, we neglected masses. To parameterize the deviation from the exact back-to-back configuration, we let $\delta\theta$ be the angle between $\mathbf{p}_{A,\gamma}$ and $-\mathbf{p}_{B,\gamma}$.

Although some issues can be treated with coordinate axes fixed in the laboratory, independent of the detected hadrons, we will find it convenient to use light-front coordinates with a z axis defined from the hadron directions. The spatial axes can be defined covariantly by normalized 4-vectors whose energy components in the CM frame are zero. For the z and x axes we choose

$$Z_\gamma^\mu = \frac{\left(0, \mathbf{n}_{A,\gamma} - \mathbf{n}_{B,\gamma}\right)}{|\mathbf{n}_{A,\gamma} - \mathbf{n}_{B,\gamma}|}, \qquad X_\gamma^\mu = \frac{\left(0, \mathbf{n}_{A,\gamma} + \mathbf{n}_{B,\gamma}\right)}{|\mathbf{n}_{A,\gamma} + \mathbf{n}_{B,\gamma}|}. \tag{13.2}$$

As shown in Fig. 13.2(b), the z axis bisects the angle between $\mathbf{p}_{A,\gamma}$ and $-\mathbf{p}_{B,\gamma}$, and the x axis is orthogonal to it in the hadron-hadron plane. Thus in the back-to-back region, Z characterizes the jet axis, and X characterizes the transverse direction of the hadron pair. The y axis is the remaining axis in a right-handed system. The time axis can be defined by $T^\mu = q^\mu/Q$.

Then we define photon-frame light-front coordinates for a vector V by

$$V_\gamma^\pm \overset{\text{def}}{=} \frac{V \cdot (T \mp Z)}{\sqrt{2}}. \tag{13.3}$$

13.2.2 Hadron frame

In the hadron frame, illustrated in Fig. 13.2(c), the detected hadrons are exactly back-to-back, but the virtual photon has a generally non-zero transverse momentum. We choose the positive z axis to be the direction of p_A, and define light-front coordinates for this frame by

$$q_h = \left(q_h^+, q_h^-, \boldsymbol{q}_{h\,\mathrm{T}}\right), \tag{13.4a}$$

$$p_{A,h} = \left(p_{A,h}^+, m_A^2/2p_{A,h}^+, \boldsymbol{0}_{\mathrm{T}}\right) \simeq \left(p_{A,h}^+, 0, \boldsymbol{0}_{\mathrm{T}}\right), \tag{13.4b}$$

$$p_{B,h} = \left(m_B^2/2p_{B,h}^-, p_{B,h}^-, \boldsymbol{0}_{\mathrm{T}}\right) \simeq \left(0, p_{B,h}^-, \boldsymbol{0}_{\mathrm{T}}\right). \tag{13.4c}$$

We define scaling variables by

$$z_A = \frac{p_{A,h}^+}{q_h^+} \simeq \frac{p_A \cdot p_B}{q \cdot p_B}, \qquad z_B = \frac{p_{B,h}^-}{q_h^-} \simeq \frac{p_A \cdot p_B}{q \cdot p_A}. \tag{13.5}$$

The photon transverse momentum in the photon frame measures how much the hadrons deviate from the back-to-back configuration in the CM frame:

$$q_{h\,\mathrm{T}}^2 = 2q_h^+ q_h^- - Q^2 \simeq \frac{2p_A \cdot q\; p_B \cdot q}{p_A \cdot p_B} - Q^2 = Q^2 \tan^2 \frac{\delta\theta}{2}. \tag{13.6}$$

Formulae for z_A, z_B, and $q_{h\,\mathrm{T}}$ in terms of Lorentz invariants can also be obtained with retention of hadron masses, but I will not present them. Our definition of the hadron frame is non-unique, in that it can be changed by a boost in the z direction, which will not affect our derivations. If necessary, the frame can be fixed by requiring the photon to have zero rapidity, i.e., $q_h^+ = q_h^-$. In the general case

$$q_h^\pm = e^{\pm y} \frac{Q}{\sqrt{2}\cos(\delta\theta/2)}. \tag{13.7}$$

13.2.3 Lorentz transformation between photon and hadron frames

The Lorentz transformation between the photon and hadron frames is

$$
\begin{aligned}
V_h = L\left(V_\gamma^+, V_\gamma^-, \boldsymbol{V}_{\gamma\,\mathrm{T}}\right) = \Bigg(& e^y \left[V_\gamma^+ \frac{\kappa+1}{2} + V_\gamma^- \frac{\kappa-1}{2} + \frac{\boldsymbol{V}_{\gamma\,\mathrm{T}} \cdot \boldsymbol{q}_{h\,\mathrm{T}}}{Q\sqrt{2}}\right], \\
& e^{-y}\left[V_\gamma^+ \frac{\kappa-1}{2} + V_\gamma^- \frac{\kappa+1}{2} + \frac{\boldsymbol{V}_{\gamma\,\mathrm{T}} \cdot \boldsymbol{q}_{h\,\mathrm{T}}}{Q\sqrt{2}}\right], \\
& \boldsymbol{V}_{\gamma\,\mathrm{T}} + \boldsymbol{q}_{h\,\mathrm{T}}\left[\frac{V_\gamma^+}{Q\sqrt{2}} + \frac{V_\gamma^-}{Q\sqrt{2}} + \frac{\boldsymbol{V}_{\gamma\,\mathrm{T}} \cdot \boldsymbol{q}_{h\,\mathrm{T}}}{Q^2(\kappa+1)}\right]\Bigg),
\end{aligned} \tag{13.8}
$$

where $\kappa = \sqrt{1 + q_{h\,\mathrm{T}}^2/Q^2} \simeq 1/\cos(\delta\theta/2)$, and y is the rapidity of q in the hadron frame, i.e., $y = \ln(q_h^+/q_h^-)$. Note carefully that although the components of V on the right-hand side of this equation are in the photon frame, the transverse vector $\boldsymbol{q}_{h\,\mathrm{T}}$ is for the photon in

the hadron frame. Note also that with the x and z axes defined in Fig. 13.2 q_h has a negative x component: $q_h^x = -Q \tan(\delta\theta/2)$, $q_h^y = 0$.

13.2.4 Structure function analysis

We make a structure function analysis by the method that Lam and Tung (1978) used for the Drell-Yan process. It starts from a hadronic tensor $W^{\mu\nu}$, which obeys current conservation, $q_\mu W^{\mu\nu} = W^{\mu\nu} q_\nu = 0$, is symmetric under $\mu \longleftrightarrow \nu$, and obeys parity conservation. When the detected hadrons have zero spin or their polarization is not measured, we have

$$W^{\mu\nu}(q, p_A, p_B) \overset{\text{def}}{=} 4\pi^3 \sum_X \delta^{(4)}(p_X + p_A + p_B - q)$$

$$\times \langle 0| j^\mu(0) | p_A, p_B, X, \text{ out} \rangle \langle p_A, p_B, X, \text{ out}| j^\nu(0) | 0 \rangle$$

$$= (-\tilde{g}^{\mu\nu} - Z^\mu Z^\nu) W_\text{T} + Z^\mu Z^\nu W_\text{L} - (X^\mu Z^\nu + Z^\mu X^\nu) W_\Delta$$

$$+ (-\tilde{g}^{\mu\nu} - 2X^\mu X^\nu - Z^\mu Z^\nu) W_{\Delta\Delta}, \tag{13.9}$$

where the structure functions W_T, etc., are functions of Lorentz invariants. We define $\tilde{g}^{\mu\nu} = g^{\mu\nu} - q^\mu q^\nu / Q^2$, and the orthogonal unit vectors Z and X were defined in (13.2).

The structure function decomposition (13.9) and the associated cross section formulae can be readily generalized to include the case of Z exchange or that the hadrons are polarized. But to explain the principles, we avoid these complications.

The names of the structure functions (T, L, Δ, and $\Delta\Delta$) characterize the corresponding polarization state of a spin-1 particle of momentum q: T is for an azimuthally symmetric transverse polarization around Z, L is for longitudinal polarization, Δ is for one unit of helicity flip in the density matrix, and $\Delta\Delta$ is for two units of helicity flip. Each gives a characteristic term in the angular dependence of the cross section:

$$E_A E_B \frac{\text{d}\sigma}{\text{d}^3 \boldsymbol{p}_A \, \text{d}^3 \boldsymbol{p}_B} = \frac{\alpha^2}{16\pi^3 Q^4} \left[(1 + \cos^2\theta) \, W_\text{T} + \sin^2\theta \, W_\text{L} \right.$$

$$\left. + \sin 2\theta \cos\phi \, W_\Delta + \sin^2\theta \cos 2\phi \, W_{\Delta\Delta} \right]. \tag{13.10}$$

Here θ is the polar angle of the leptons with respect to the Z direction, and ϕ is the azimuthal angle around Z, with the direction X corresponding to $\phi = 0$. The angular dependence corresponds to the angular momentum associated with each structure function.

Some confusion about the azimuthal angle can be avoided by realizing that there are actually two azimuthal angles that can be measured from the two hadrons, but that the cross section (13.10) only depends on one of them. In the overall CM frame with the incoming lepton beams along the z axis, these angles can be characterized as (a) the azimuthal angle of the overall jet axis Z^μ relative to some fixed axis, and (b) the azimuthal angle of the hadron plane relative to the plane that contains Z^μ and the leptons. The dependence is on the second angle, but not the first. The reason for this is that because the leptons are unpolarized, the initial state has nothing to allow an intrinsic azimuthal axis to be defined.

There are "kinematic zeros" in W_Δ and $W_{\Delta\Delta}$ at $q_{h\,\mathrm{T}} = 0$, since the dependence on the direction X arises only from the transverse momentum $\boldsymbol{q}_{h\,\mathrm{T}}$. So when $q_{h\,\mathrm{T}} \to 0$, W_Δ is proportional to $q_{h\,\mathrm{T}}$ and $W_{\Delta\Delta}$ is proportional to $q_{h\,\mathrm{T}}^2$.

13.3 Region analysis

We now start the derivation of a factorization property suitable for the case of relatively low transverse momentum, i.e., $q_{h\,\mathrm{T}} \ll Q$. Later we will combine this with a more standard factorization for large transverse momentum to give a result valid for all $q_{h\,\mathrm{T}}$. We will assume throughout that the hadron energies in the CM frame are comparable with Q. That is, we do not treat the case of very small values for the scaling variables z_A and z_B.

The strategy was already explained in Chs. 10 and 12. One feature critical to a proper derivation is the use of the integral of the hadronic tensor with a test function, as in (12.11); this allows a clean understanding of the accuracy of the region approximants. Another feature is a shift between hadron and photon frames in defining the hadron scattering; this will give consistency of parton kinematics between fragmentation functions and perturbative calculations of the hard scattering.

13.3.1 Only two jets

Since we assume that the observed hadrons H_A and H_B have energies of order Q, they are part of jet subgraphs, not of the soft subgraph, in the leading regions. As already explained in Sec. 13.1, the leading regions when $q_{h\,\mathrm{T}} \ll Q$ have only have two jet subgraphs, as in Fig. 13.1; regions with three or more jet subgraphs are suppressed by a power of $q_{h\,\mathrm{T}}/Q$.

13.3.2 Region approximators

In the subtraction formalism, Sec. 10.1, the contribution of a particular region R of a graph is obtained by applying an approximator T_R to the graph. But it is applied only after subtractions are made for smaller regions, to avoid double-counting problems.

For reasons already encountered in Secs. 12.7 and 12.8, we apply the approximators not to the hadronic tensor $W^{\mu\nu}$ itself, but to an integral of it with a test function. The integral, $W^{\mu\nu}([f], p_A, p_B)$, is defined just as in (12.11) for the one-particle-inclusive case. The argument of the test function is the sum of the collinear and soft momenta in the final state: $f(k_A + k_B + k_S)$. Region approximants are applied to internal virtual lines of collinear and hard subgraphs, and to the argument of the test function.

If, instead, the approximant were used for the unintegrated $W^{\mu\nu}$, it would be applied to soft momenta circulating through final states of collinear subgraphs. The errors associated with approximants that directly change the final-state momenta are hard to control.

The approximant for a soft momenta in a collinear subgraph is unchanged from that in Sec. 10.4.2 for the Sudakov form factor. The approximant is also unchanged from the one for single-particle-inclusive e^+e^- annihilation in Sec. 12.8.1, except for the choice of the

directions defining the auxiliary vectors. These are now derived from the momenta of the observed hadrons, and we apply the definitions in the hadron frame using the light-front coordinates defined in (13.4).

The approximants for soft and collinear momenta in the hard subgraphs have an apparently small but very significant change compared with (10.19) for the Sudakov form factor. This concerns the frames used to specify the light-like auxiliary vectors. We now define the projectors for collinear momenta into the hard subgraph by

$$P_{HA}(k_A) = \frac{w_{HA}\, k_A \cdot w_B}{w_{HA} \cdot w_B}, \qquad P_{HB}(k_B) = \frac{w_{HB}\, k_B \cdot w_A}{w_{HB} \cdot w_A}. \tag{13.11}$$

Here w_A and w_B are light-like vectors defined in the hadron frame: $w_{A,h} = (1, 0, \mathbf{0}_\mathrm{T})$ and $w_{B,h} = (0, 1, \mathbf{0}_\mathrm{T})$. They correspond to vectors used in the soft-to-collinear approximants and in the definitions of fragmentation functions. But for reasons to be explained below, the other vectors are defined in photon frame: $w_{HA,\gamma} = (1, 0, \mathbf{0}_\mathrm{T})$ and $w_{HB,\gamma} = (0, 1, \mathbf{0}_\mathrm{T})$.

As with the Sudakov form factor, a momentum from a collinear subgraph may include a circulating soft component. This is approximated, to be in direction w_B in collinear subgraph $C_{(A)}$, and in direction w_A in collinear subgraph $C_{(B)}$. From (13.11), these circulating soft momenta are replaced by zero in the hard scattering, as for the Sudakov form factor.

The reason for the new definitions of the projectors is that we normally perform perturbative calculations of the hard scattering in the photon frame, where the virtual photon has zero transverse momentum. Thus the calculations correspond to the elastic process $e^+e^- \to q\bar{q}$ in its CM frame. Therefore we arrange that in the photon frame the approximated quark momenta are in the plus and minus directions. This complication did not arise for the Sudakov form factor, since it is an elastic process, for which the photon and hadron frames coincide.

In hadron-frame components, the approximated momenta are

$$P_{HA}(k_A)_h = k_{A,h}^+ \left(1, \; e^{-2y}\frac{\kappa - 1}{\kappa + 1}, \; e^{-y}\frac{\mathbf{q}_{h\,\mathrm{T}}\sqrt{2}}{Q(\kappa + 1)}\right), \tag{13.12a}$$

$$P_{HB}(k_B)_h = k_{B,h}^- \left(e^{2y}\frac{\kappa - 1}{\kappa + 1}, \; 1, \; e^{y}\frac{\mathbf{q}_{h\,\mathrm{T}}\sqrt{2}}{Q(\kappa + 1)}\right). \tag{13.12b}$$

Note that these leave unchanged the "large components", i.e., $k_{A,h}^+$ and $k_{B,h}^-$. The photon-frame components are

$$P_{HA}(k_A)_\gamma = \frac{2e^{-y}k_{A,h}^+}{1 + \kappa}\left(1, 0, \mathbf{0}_\mathrm{T}\right), \quad P_{HB}(k_B)_\gamma = \frac{2e^{y}k_{B,h}^-}{1 + \kappa}\left(0, 1, \mathbf{0}_\mathrm{T}\right). \tag{13.13}$$

These formulae apply not just to the total collinear momenta entering the hard subgraph, but equally to the individual momenta on particular external lines of H. Let these momenta be indicated by an index j: k_{Aj}, k_{Bj}. Then, by momentum conservation at the hard scattering,

the virtual photon's momentum in the photon frame is changed to

$$\hat{q}_\gamma = \left(\sum_j k_{Aj,h}^+ e^{-y}, \sum_j k_{Bj,h}^- e^y, \mathbf{0}_T \right) \frac{2}{\kappa + 1}. \tag{13.14}$$

To restore the original value of q, we will define an approximant on the test function, in (13.18) below. In effect, this approximant will change the momentum of the final state relative to q.

Dirac projectors on the external lines of the hard subgraphs need to be modified from those defined in Sec. 10.4.2. For quark lines between C_A and H we use

$$\mathcal{P}_A \overset{\text{def}}{=} \frac{\gamma \cdot w_{HA} \gamma \cdot w_B}{2 w_B \cdot w_{HA}}, \qquad \overline{\mathcal{P}}_A \overset{\text{def}}{=} \frac{\gamma \cdot w_B \gamma \cdot w_{HA}}{2 w_B \cdot w_{HA}}, \tag{13.15}$$

and for quark lines between C_B and H we use

$$\mathcal{P}_B \overset{\text{def}}{=} \frac{\gamma \cdot w_{HB} \gamma \cdot w_A}{2 w_A \cdot w_{HB}}, \qquad \overline{\mathcal{P}}_B \overset{\text{def}}{=} \frac{\gamma \cdot w_A \gamma \cdot w_{HB}}{2 w_A \cdot w_{HB}}. \tag{13.16}$$

On the side next to the hard scattering, the factors $\gamma \cdot w_{HA}$ and $\gamma \cdot w_{HB}$ project onto wave functions for the (approximated) massless on-shell quarks. On the side next to the collinear subgraphs, the factors $\gamma \cdot w_A$ and $\gamma \cdot w_B$ project onto the components of the Dirac fields that are used in the hadron-frame definitions of fragmentation functions. As usual, we use the Dirac conjugation notation: $\overline{\Gamma} \overset{\text{def}}{=} \gamma^0 \Gamma^\dagger \gamma^0$.

In the approximant in the test function we must preserve the exact transverse momentum of the collinear and soft partons, since we wish to obtain a cross section differential in $\mathbf{q}_{h\,T}$.

Previously, in the one-particle-inclusive cross section, the approximator made the replacement

$$f(k_A + k_B + k_S) \mapsto f(k_A^+, k_B^-, \mathbf{0}_T), \quad \text{(previous)} \tag{13.17}$$

where we neglected not only the small longitudinal components k_A^- and k_B^+, but also all the transverse momenta. For TMD factorization, we must change the approximant to retain the transverse momenta. But to keep the longitudinal components consistent with those required by momentum conservation in the hard scattering, we apply a scaling to the plus and minus components of k_A and k_B. We therefore define the approximant on the test function in terms of hadron-frame momenta by

$$f(k_{A,h} + k_{B,h} + k_{S,h}) \mapsto f\left(k_{A,h}^+ \frac{2\kappa}{\kappa + 1}, k_{B,h}^- \frac{2\kappa}{\kappa + 1}, \mathbf{k}_{A,h\,T} + \mathbf{k}_{B,h\,T} + \mathbf{k}_{S,h\,T} \right). \tag{13.18}$$

The scaling factor $2\kappa/(\kappa + 1) = 2/(1 + \cos(\delta\theta/2))$ is, of course, unity in the limit that $q_{h\,T}$ is zero. It is chosen so that after the next step of functional differentiation, $\hat{q}_\gamma$ in (13.14) reproduces q, i.e., the hard scattering has the original value of q.

To find the actual hadronic tensor $W^{\mu\nu}(q, p_A, p_B)$, we functionally differentiate the integrated tensor with respect to the test function f:

$$W^{\mu\nu}(q, p_A, p_B) = \frac{\delta W^{\mu\nu}([f], p_A, p_B)}{\delta f(q)}. \tag{13.19}$$

The result is that the approximated parton momenta, in (13.18), sum to q. Relative to an unapproximated graph, the transverse momenta are unchanged, but the longitudinal momenta are shifted by amounts that are power-suppressed in the design region of the approximator. This results in power-suppressed errors in the hadronic tensor itself, provided that scale of the $q_h^{\pm}$ dependence of the hadronic tensor is Q rather than a smaller scale.

As usual, the internal integrations are over all momenta. Outside the design region R of approximator T_R, the accuracy of the approximation degrades. But this is handled by terms for larger regions than R, combined with the double-counting subtractions in the subtraction method.

13.3.3 Ward identities

There is no change in the Ward identities that extract K gluons from hard and collinear subgraphs and that led to Fig. 12.12. There are now only two collinear subgraphs, so the hard scattering only has two external lines, and each collinear subgraph has a detected hadron.

At this point the color flow is as shown in Fig. 12.13. We now disentangle the color flow between the various factors. As before, the collinear factors are color-singlet, so we convert to the form of Fig. 12.15, where the sums over the color indices of the hard scattering bypass the collinear factors, which are now defined with a color average.

In our two-collinear-subgraph case, the entangled hard-soft combination has color sums of the form

$$H_{ab} S_{ab;a'b'} H^*_{a'b'}, \tag{13.20}$$

with repeated indices summed. Since the hard-scattering amplitudes are color-singlet, we replace this by

$$\left(H_{ab} H^*_{ab} \right) \frac{1}{N_c} S_{cc;dd}. \tag{13.21}$$

Here there is a color trace for the hard scattering, the same as in a cross section with a sum over final-state color, while the soft factor is color averaged. So from Fig. 12.12 we obtain Fig. 13.3, where each of the collinear and soft factors has a color average. The collinear and hard factors are still linked by a Dirac trace that we will analyze later.

As usual, a sum over graphs and regions converts Fig. 13.3 to a factorization formula. The operator definitions for the factors are determined by the approximants, and there are appropriate double-counting subtractions in the factors. The factorized form is

$$W^{\mu\nu} = 4\pi^3 z_A z_B \sum_f \int d^2\boldsymbol{k}_{A\,\mathrm{T}}\, d^2\boldsymbol{k}_{B\,\mathrm{T}}\ S(\boldsymbol{q}_{h\,\mathrm{T}} - \boldsymbol{k}_{A\,\mathrm{T}} - \boldsymbol{k}_{B\,\mathrm{T}})$$

$$\times \operatorname{Tr} \mathcal{P}_A\, C_A(z_A, \boldsymbol{k}_{A\,\mathrm{T}}; f) \overline{\mathcal{P}}_A\ H^\nu_f\, \mathcal{P}_B\, C_B(z_B, \boldsymbol{k}_{B\,\mathrm{T}}; \bar{f}) \overline{\mathcal{P}}_B\ \overline{H}^\mu_f(Q), \tag{13.22}$$
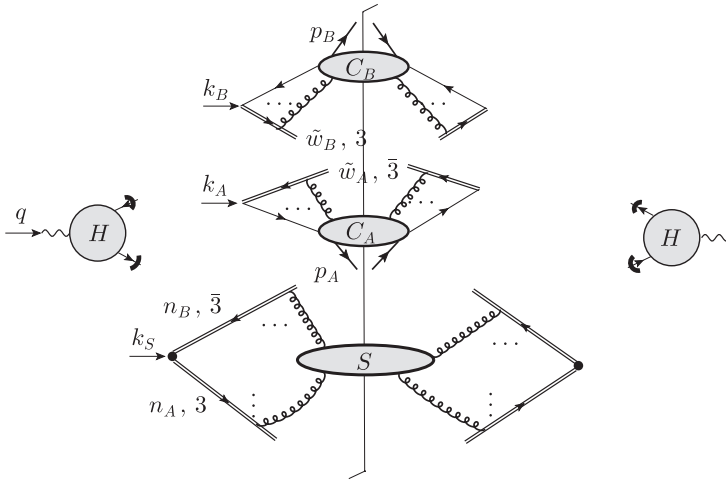
Fig. 13.3. Same as Fig. 12.12, but for two-hadron-inclusive cross section in the back-to-back region. The color flow has been reorganized: the collinear and soft factors have color averages, and there is a color trace between the hard-scattering amplitudes on the left and the right of the final-state cut.

where all transverse momenta are in the hadron frame, the Dirac projectors were defined in (13.15) and (13.16), and the factors S, C_A, and C_B will be defined below. The sum over f is over the flavors of quark and antiquark that can enter the C_A factor, i.e., u, $\bar{u}$, d, $\bar{d}$, etc.; the opposite flavor is used for C_B.

The following steps give the above formula.

1. We perform the functional differentiation, (13.19), for the approximated $W^{\mu\nu}$. This sets the transverse momentum in the soft factor equal to $\boldsymbol{q}_{h\,\mathrm{T}} - \boldsymbol{k}_{A,h\,\mathrm{T}} - \boldsymbol{k}_{B,h\,\mathrm{T}}$. It also sets $k_{A,h}^+ = q_h^+$ and $k_{B,h}^- = q_h^-$ in the collinear factors C_A and C_B.
2. The approximation removed dependence of the test function on $k_{A,h}^-$, $k_{B,h}^+$, and $k_{S,h}^{\pm}$. So the integrals over these variables are "short-circuited" and included in the definitions of C_A, C_B, and S.
3. The soft factor is $S = Z_S S_{(0)}$, which is a UV-renormalization factor $Z_S(y_A - y_B, g, \epsilon)$ times a bare soft factor

$$S_{(0)}(\boldsymbol{k}_{S\,\mathrm{T}}) = \frac{1}{N_c} \int \frac{\mathrm{d}k_S^+ \, \mathrm{d}k_S^-}{(2\pi)^{4-2\epsilon}} \quad \text{} \tag{13.23}$$

The Wilson lines are in non-light-like directions defined as in Sec. 12.8.1, but now using the hadron frame: $n_{A,h} = (1, -e^{-2y_A}, \boldsymbol{0}_{\mathrm{T}})$, $n_{B,h} = (-e^{2y_B}, 1, \boldsymbol{0}_{\mathrm{T}})$. The rapidities and light-front coordinates for the two collinear subgraphs are in the hadron frame, rather
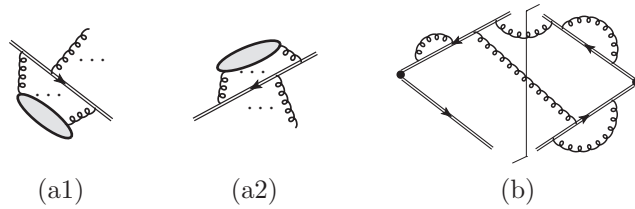
Fig. 13.4. (a1) and (a2) Omitted from (13.23) are graphs containing Wilson-line self-interaction structures of this kind. (b) Example of omitted graph with four of the prohibited structures.

than being in the different collinear-subgraph-specific coordinates used in Sec. 12.8.1. There is a color trace over the Wilson lines, and, as explained above, there is a factor $1/N_c$ to give a color average.

The Wilson lines are obtained by the Ward-identity argument, given in Sec. 11.9. But this does not produce graphs that contain a subgraph connecting only to one of the straight-line segments of the Wilson line. Thus graphs containing structures like those in Fig. 13.4 are omitted; this is indicated by the subscript "no SI" (for "no self-interaction"). More details are given in Sec. 13.3.4.

4. The collinear factor C_A is defined with the integral

$$\frac{k_{A,h}^+}{p_{A,h}^+} \int \frac{\mathrm{d}k_{A,h}^-}{(2\pi)^{4-2\epsilon}}, \qquad (13.24)$$

as appropriate for a fragmentation function; see (12.39).

5. The longitudinal momentum fraction in C_A is then

$$\frac{p_{A,h}^+}{k_{A,h}^+} = z_A \frac{2}{\kappa + 1}. \qquad (13.25)$$

Now the factor $2/(\kappa + 1)$ goes to unity in the limit $q_{h\,\mathrm{T}}/Q \to 0$, and the approximations used elsewhere in the derivation are only valid only to leading power in $q_{h\,\mathrm{T}}/Q$. So we replaced the momentum fraction by z_A in (13.22).

Corrections will handled by methods appropriate to the large transverse momentum region, in Sec. 13.12.

6. As in the Sudakov form factor, soft subtractions are applied to the collinear factors.
7. The same methods give the other collinear factor C_B.
8. A prefactor of $z_A z_B$ compensates factors of $1/z_A$ and $1/z_B$ in the definitions of the fragmentation functions, as in (13.24). Those factors normalize the fragmentation functions like number densities.
9. The Dirac and color traces are explicit in (13.22) rather than being absorbed into the fragmentation functions.

As for determining the Wilson lines and implementing the soft subtractions in the collinear factors: In Sec. 13.6, we will use Fourier transforms on transverse momenta to

convert the convolution in transverse momentum in (13.22) to a product in transverse position space. After that, the arguments we used in Ch. 10 for the Sudakov form factor apply in the same way here to determine appropriate directions for the Wilson lines, and to find optimal definitions of the factors.

We will determine the allowed polarization dependence of the fragmentation functions, after which we will determine the angular distribution, with an interesting correction to the standard $1 + \cos^2 \theta$ form.

13.3.4 Wilson-line self-interactions

As already remarked, Wilson-line self-interactions, Fig. 13.4, are omitted from the definition of the soft factor, (13.23). We met exactly the same issue in an abelian theory, e.g., in (10.89). But in an abelian theory, the Wilson lines could be simplified, by the use of (10.100), to replace the sum over gluon attachments to a Wilson line by a product of single Wilson-line propagators. Then the self-interactions of the Wilson lines could be factored out. A simple factorization of Wilson-line self-interactions does not work in a non-abelian theory.

An immediate consequence is that despite being defined from a matrix element of a Wilson-line operator, the soft factor depends on the gauge used to formulate the theory; a gauge-dependent set of graphs is omitted. Similar issues apply to the collinear factors.

These problems will be solved by a reorganization of the factorization formula in Sec. 13.7, just as for the Sudakov form factor in Sec. 10.11.

13.4 Collinear factors

There are two parts to our treatment of the collinear factors, leading to definitions of fragmentation functions. In this section, we treat quark polarization and the azimuthal dependence of the fragmentation functions. The second part, in Sec. 13.7, concerns the Wilson lines.

13.4.1 Quark fragmentation, including polarization

The Dirac projectors for the leading power restrict the collinear factor C_A to terms proportional to γ^-, $\gamma^- \gamma_5$, and $\gamma^- \gamma^i$ (with i a *transverse* index). Given that we choose the observed hadrons to be spinless, the $\gamma^- \gamma_5$ term is prohibited by parity invariance. For an *integrated* fragmentation function, the $\gamma^- \gamma^i$ term is prohibited by invariance under rotations about the z axis. But for an unintegrated fragmentation function, the quantity C_A can have a term $\gamma^- \gamma^i \boldsymbol{k}^i_{A,h\,\mathrm{T}}$ times a function of the size of $\boldsymbol{k}_{A,h\,\mathrm{T}}$.

We now recall our results in Sec. 12.4.7, and use them to convert (13.22) to use fragmentation functions that allow for quark polarization. Given the longitudinal and transverse polarization of the initial quark, we must project the trace of C_A as indicated in (12.41a).

The first term on the r.h.s. of (12.41a) gives the unpolarized fragmentation function, which is independent of the azimuthal angle of the quark's transverse momentum. The second term goes with a factor that is zero by parity invariance. The trace with the third term picks out the $\gamma^-\gamma^i k^i_{A\,\mathrm{T}}$ term in C_A,

$$-\mathrm{Tr}\,\gamma^-\sum_{i=1,2}\gamma^i \boldsymbol{k}^i_{A,h\,\mathrm{T}}\gamma^+\sum_{j=1,2}\gamma_5\gamma^j s^j_\mathrm{T}$$

$$= 4i(k^x_{A,h\,\mathrm{T}}s^y_\mathrm{T} - k^y_{A,h\,\mathrm{T}}s^x_\mathrm{T}) = 4i|\boldsymbol{k}_{A,h\,\mathrm{T}}||\boldsymbol{s}_\mathrm{T}|\sin(\phi_s - \phi_k), \qquad (13.26)$$

where ϕ_s and ϕ_k are the azimuthal angles of $\boldsymbol{s}_\mathrm{T}$ and $\boldsymbol{k}_{A,h\,\mathrm{T}}$. The result is a characteristic angular dependence, which we will relate to the angular dependence of the two-hadron-inclusive cross section. In this equation, superscripts x and y are used for transverse components. The transverse spin vector $\boldsymbol{s}_\mathrm{T}$ of the quark will be obtained from calculations of the hard scattering in the photon frame. But it can be verified from the form of the Dirac projector $\mathcal{P}_A$ that the same numerical vector can be applied in the hadron frame.

The basic derivation just given applies in a model field theory without gauge fields. In a gauge theory, Wilson lines need to be attached to the quark fields. Since the Wilson lines are chosen to be in the (t, z) plane, they do not affect any azimuthal dependence. So we can apply the same Dirac trace in full QCD.

The factorization formula (13.22) has transverse momentum for the quark, and zero transverse momentum for the hadron. But the number-density interpretation is in terms of a transverse momentum of the hadron relative to the quark, as given by (12.34a), so fragmentation functions are treated as functions of z_j and $\boldsymbol{p}_{j\,\mathrm{T}}$, where

$$\boldsymbol{p}_{j\,\mathrm{T}} = -z_j \boldsymbol{k}_{j,h\,\mathrm{T}}. \qquad (13.27)$$

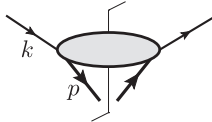*Don't forget the minus sign in this relation!*

The resulting fragmentation function $d_{h/f}(z, \boldsymbol{p}_\mathrm{T})$ depends on the azimuthal angle of the transverse momentum. We decompose it into azimuth-independent fragmentation functions, which we normalize by the Trento conventions (Bacchetta *et al.*, 2004),

$$d_{h/f}(z, \boldsymbol{p}_\mathrm{T}) = D_{1,\,h/f}(z, p_\mathrm{T}) + H^\perp_{1,\,h/f}(z, p_\mathrm{T})\frac{p^x_{h\,\mathrm{T}}s^y_\mathrm{T} - p^y_{h\,\mathrm{T}}s^x_\mathrm{T}}{zM_h}$$

$$= D_{1,\,h/f}(z, p_\mathrm{T}) + H^\perp_{1,\,h/f}(z, p_\mathrm{T})\frac{|\boldsymbol{s}_\mathrm{T}||\boldsymbol{p}_{h\,\mathrm{T}}|}{zM_h}\sin(\phi_h - \phi_s), \qquad (13.28)$$

where the notations D_1 and $H^\perp_1$ are those of Mulders and Tangerman (1996), M_h is the mass of the detected hadron, and ϕ_h and ϕ_s are the azimuths of the hadron and the quark spin. Note that the ϵ tensor in Bacchetta *et al.* (2004) has the opposite sign to the one used in this book, so I have avoided using it in (13.28).

We therefore have two TMD fragmentation functions. Without the Wilson lines, the unpolarized one is defined by (12.39), but we now use the symbol D_1 instead of d. The

polarized fragmentation function is

$$H_{1,\,h/f}^{\perp}(z,\,p_{\mathrm{T}}) \frac{p_{\mathrm{T}}^x s_{\mathrm{T}}^y - p_{\mathrm{T}}^y s_{\mathrm{T}}^x}{z M_h}$$

$$\overset{\text{prelim}}{=} -\frac{\mathrm{Tr}_{\text{color}}}{N_{c,f}} \frac{\mathrm{Tr}_{\text{Dirac}}}{4} \sum_X \frac{1}{z} \int \frac{\mathrm{d}x^- \,\mathrm{d}^{n-2}\boldsymbol{x}_{\mathrm{T}}}{(2\pi)^{n-1}} e^{i k_h^+ x^- - i \boldsymbol{k}_{h\,\mathrm{T}} \cdot \boldsymbol{x}_{\mathrm{T}}}$$

$$\times \gamma^+ \gamma_5 \boldsymbol{\gamma}_{\mathrm{T}} \cdot \boldsymbol{s}_{\mathrm{T}} \langle 0| \psi_j^{(0)}(x/2)| p, X, \text{ out}\rangle \langle p, X, \text{ out}| \bar{\psi}_j^{(0)}(-x/2)|0\rangle$$

$$= -\frac{\mathrm{Tr}_{\text{color}}}{N_{c,j}} \frac{\mathrm{Tr}_{\text{Dirac}}}{4} \frac{1}{z} \int \frac{\mathrm{d}k^-}{(2\pi)^n} \gamma^+ \gamma_5 \boldsymbol{\gamma}_{\mathrm{T}} \cdot \boldsymbol{s}_{\mathrm{T}} \qquad \text{(13.29)}$$

where the overall minus sign is from the third term on the r.h.s. of (12.41a). $H_{1,\,h/f}^{\perp}$ is commonly called the Collins function (Collins, 1993). Its physical importance is that it gives a correlation between the azimuthal distribution of a hadron and the transverse spin of its parent quark. It therefore provides a measure of the quark polarization. The "prelim" designation of this definition is a reminder that we have not yet included Wilson lines.

13.4.2 Antiquark fragmentation

Exchanging the quark and antiquark lines in the above definition gives the Collins function for an antiquark. From (12.41) it follows that no change of sign is needed.

13.4.3 Coordinate systems for C_A and C_B factors

The above definitions apply to the fragmentation functions corresponding to C_A in (13.22). But an exchange of the roles of the plus and minus axes, i.e., a reversal of the z axis is necessary for the C_B factor. Since the x, y, and z axes form a right-handed coordinate system, certain signs will reverse in obtaining the polarized fragmentation function.

13.4.4 Positivity and Collins function

In the absence of Wilson lines, the fragmentation function is positive, as follows from the general definition (12.35). This must apply for any polarization state of the quark in (13.28). Hence the Collins function is restricted to obey

$$\frac{|H_{1,\,h/f}^{\perp}(z,\,p_{\mathrm{T}})||\boldsymbol{p}_{h\,\mathrm{T}}|}{z M_h} \le D_{1,\,h/f}(z,\,p_{\mathrm{T}}). \qquad \text{(13.30)}$$

When we use the full QCD definitions with subtractions to prevent double counting with the soft factor, we may find some violation of this constraint.

13.5 Initial version of factorization with TMD fragmentation

13.5.1 Factorization

We now express (13.22) in terms of the fragmentation functions:

$$
W^{\mu\nu} \overset{\text{prelim}}{=} \frac{8\pi^3 z_A z_B}{Q^2} \sum_f \int d^2 \boldsymbol{k}_{A,h\,T}\, d^2 \boldsymbol{k}_{B,h\,T}\; S(\boldsymbol{q}_{h\,T} - \boldsymbol{k}_{A\,T} - \boldsymbol{k}_{B\,T})
$$

$$
\times\, D_{1,\,H_A/f}(z_A, z_A k_{A,h\,T})\, D_{1,\,H_B/\bar{f}}(z_B, z_B k_{B,h\,T})
$$

$$
\times \operatorname{Tr} k_{A,\gamma}^+ \gamma^- (1 - \gamma_5 \boldsymbol{\gamma}_T \cdot \boldsymbol{a}_{A,\gamma\,T}) H_f^\nu(Q) k_{B,\gamma}^- \gamma^+ (1 - \gamma_5 \boldsymbol{\gamma}_T \cdot \boldsymbol{a}_{B,\gamma\,T}) \overline{H}_f^\mu(Q). \tag{13.31}
$$

The "prelim" notation is used because we will modify the definitions of the factors to get our final factorization formula. The Collins function appears in the transverse vectors $\boldsymbol{a}_{A\,T}$ and $\boldsymbol{a}_{B\,T}$ defined by

$$
\boldsymbol{a}_{A,\gamma\,T} \overset{\text{def}}{=} \left(+ k_{A,h\,T}^y,\; -k_{A,h\,T}^x \right) \alpha_A, \tag{13.32a}
$$

$$
\boldsymbol{a}_{B,\gamma\,T} \overset{\text{def}}{=} \left(- k_{B,h\,T}^y,\; +k_{B,h\,T}^x \right) \alpha_B, \tag{13.32b}
$$

where the scalar coefficients are

$$
\alpha(z, zk_{h\,T}; h/f) \overset{\text{def}}{=} \frac{H_{1,\,h/f}^\perp(z, zk_{h\,T})}{M_h D_{1,\,h/f}(z, zk_{h\,T})}, \tag{13.33}
$$

and the reversed sign between the definitions of $\boldsymbol{a}_{A,\gamma\,T}$ and $\boldsymbol{a}_{B,\gamma\,T}$ allows for the reversed z axis in the definitions of the fragmentation functions between the two collinear subgraphs.

The scalar coefficients α_A and α_B have the dimensions of inverse mass, and quantify the Collins function relative to unpolarized fragmentation. The vectors $\boldsymbol{a}_{j,\gamma\,T}$ are the analyzing power of single-particle fragmentation for measuring the transverse spin of a quark. The transverse momenta for the quarks on the r.h.s. of (13.32) are in the hadron frame. But the numerical values of the resulting transverse vectors $\boldsymbol{a}_{j,\gamma\,T}$ on the l.h.s. are treated as photon-frame vectors to be combined with the calculation of the hard scattering, performed in the photon frame.

Note: In (13.31) there is a γ_5 factor multiplying each $a_{j\,T}$ vector, thereby allowing the interpretation in terms of an analyzing power for transverse spin. But the formulae can also be expressed without the γ_5 in terms of transverse momenta, which is a convenience in calculations with loop graphs with dimensional regularization.

13.5.2 Lowest-order (LO) calculation

The hard-scattering factor in (13.31) is easily calculated at LO. We now use the photon frame, in which the quark labeled A goes in the $+z$ direction and has energy $Q/2$. The LO

hard scattering is

$$\mathrm{Tr}\, k_A^+ \gamma^- (1 - \gamma_5 \boldsymbol{\gamma}_\mathrm{T} \cdot \boldsymbol{a}_{A\mathrm{T}})\, H_f^\nu(Q)\, k_B^- \gamma^+ (1 - \gamma_5 \boldsymbol{\gamma}_\mathrm{T} \cdot \boldsymbol{a}_{B\mathrm{T}})\, \overline{H}_f^\mu(Q)$$

$$\overset{\mathrm{LO}}{=} e_f^2\, \mathrm{Tr}\, k_A^+ \gamma^- (1 - \gamma_5 \boldsymbol{\gamma}_\mathrm{T} \cdot \boldsymbol{a}_{A\mathrm{T}})\, \gamma^\nu\, k_B^- \gamma^+ (1 - \gamma_5 \boldsymbol{\gamma}_\mathrm{T} \cdot \boldsymbol{a}_{B\mathrm{T}})\, \gamma^\mu$$

$$= 2 e_f^2 Q^2 \left[\delta_\mathrm{T}^{\mu\nu} + (\delta_\mathrm{T}^{\mu\nu} \boldsymbol{a}_{A\mathrm{T}} \cdot \boldsymbol{a}_{B\mathrm{T}} - a_{A\mathrm{T}}^\mu a_{B\mathrm{T}}^\nu - a_{B\mathrm{T}}^\mu a_{A\mathrm{T}}^\nu) \right]$$

$$= 2 e_f^2 Q^2 \left[\delta_\mathrm{T}^{\mu\nu} + \alpha_A \alpha_B (\delta_\mathrm{T}^{\mu\nu} \boldsymbol{k}_{A\mathrm{T}} \cdot \boldsymbol{k}_{B\mathrm{T}} - k_{A\mathrm{T}}^\mu k_{B\mathrm{T}}^\nu - k_{B\mathrm{T}}^\mu k_{A\mathrm{T}}^\nu) \right], \tag{13.34}$$

where $\delta_\mathrm{T}^{\mu\nu}$ is a transverse Kronecker delta, the same as $-\tilde{g}^{\mu\nu} - Z^\mu Z^\nu$ in the structure function definition (13.9). Note that the dependence on $\boldsymbol{a}_{A\mathrm{T}}$ and $\boldsymbol{a}_{B\mathrm{T}}$ is only on a product of both. This implies that the quark and antiquark are individually unpolarized, but that their spins are correlated; the spin state is thus an entangled state. In the last line of (13.34), we used the definitions (13.32).

To find the results for the structure functions, defined in (13.9), we insert (13.34) in the factorization formula, and integrate over quark transverse momentum. The unpolarized term in (13.34) contributes to W_T only, giving the well-known $1 + \cos^2 \theta$ distribution associated with a spin-$\frac{1}{2}$ quark. Comparison of the spin-dependent tensor in (13.34) with the structure function decomposition shows that it gives a contribution to the $W_{\Delta\Delta}$ structure function. This gives rise to a characteristic $\cos 2\phi$ azimuthal dependence in the cross section, (13.10).

13.5.3 Lack of single-quark polarization

The lack of transverse polarization of each single quark is actually a result valid to all orders of perturbation theory. The general proof uses chirality conservation in massless perturbation theory, and is made by the argument associated with (8.84) in DIS.

13.6 Factorization and transverse coordinate space

In this section, I will restrict attention to the unpolarized term in the factorization formula. The extension to the remaining term is left as an exercise (problem 13.6).

By using a Fourier transform, we can diagonalize the convolutions over transverse momentum in the factorization formula, (13.31), and in the evolution equations to be discussed later. So we define

$$\tilde{S}(b_\mathrm{T}) = \int \mathrm{d}^{2-2\epsilon} \boldsymbol{k}_\mathrm{T}\, e^{i \boldsymbol{k}_\mathrm{T} \cdot \boldsymbol{b}_\mathrm{T}}\, S(k_\mathrm{T}), \tag{13.35a}$$

$$\tilde{D}_{1,\,h/f}(z, b_\mathrm{T}) = \int \mathrm{d}^{2-2\epsilon} \boldsymbol{k}_\mathrm{T}\, e^{i \boldsymbol{k}_\mathrm{T} \cdot \boldsymbol{b}_\mathrm{T}}\, D_{1,\,h/f}(z, z k_\mathrm{T}), \tag{13.35b}$$

etc. The normalizations differ from those in Collins and Soper (1982b). The lack of a $1/(2\pi)^{2-2\epsilon}$ normally associated with $\boldsymbol{k}_\mathrm{T}$ integral is because this factor is already in the definition of a fragmentation function. Although the phenomenological use of factorization is in four space-time dimensions, the above formulae are written in a general space-time
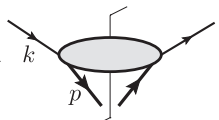
dimension, because we will also use them in dimensionally regulated perturbative calculations. All the transverse vectors are in the hadron frame.

Applying the limit $b_{\mathrm{T}} \to 0$ naively, gives the integrated fragmentation function up to normalization factor:

$$\tilde{D}_{1,\,h/f}(z, 0_{\mathrm{T}}) \stackrel{?}{=} \frac{1}{z^2} d_{h/f}(z) \text{ (at } \epsilon = 0). \tag{13.36}$$

The factor $1/z^2$ (or $z^{-2+2\epsilon}$ in a general space-time dimension $4 - 2\epsilon$) is from the scaling between parton and hadron transverse momentum, (13.27). The above result applies in a super-renormalizable non-gauge theory, and is the equivalent of (6.75) for a parton density.

Applying (13.35b) to the definition (12.39) gives

$$\tilde{D}_{1,\,h/f}(z, b_{\mathrm{T}}) \stackrel{\text{prelim}}{=} \frac{\mathrm{Tr}_{\mathrm{color}}}{N_{c,j}} \frac{\mathrm{Tr}_{\mathrm{Dirac}}}{4} \sum_X \frac{1}{z} \int \frac{\mathrm{d}x^-}{2\pi} e^{ik^+ x^-}$$

$$\times \langle 0 | \gamma^+ \psi_j^{(0)}(x/2) | p, X, \text{ out} \rangle \langle p, X, \text{ out} | \bar{\psi}_j^{(0)}(-x/2) | 0 \rangle$$

$$= \frac{\mathrm{Tr}_{\mathrm{color}}}{N_{c,j}} \frac{\mathrm{Tr}_{\mathrm{Dirac}}}{4} \frac{1}{z} \int \frac{\mathrm{d}k^- \, \mathrm{d}^{n-2} k_{\mathrm{T}}}{(2\pi)^n} e^{ik_{\mathrm{T}} \cdot b_{\mathrm{T}}} \gamma^+ \tag{13.37}$$

where the vector x is $(0, x^-, b_{\mathrm{T}})$. Thus the transverse coordinate b_{T} in the Fourier transform is exactly the transverse separation of the quark and antiquark fields. *The "prelim" notation alerts us that we have not yet explicitly treated the Wilson-line issues in the definition.* The orientation of the diagram corresponds to hadron p_A in Fig. 13.1.

Then the factorization formula becomes

$$W^{\mu\nu} \stackrel{\text{prelim}}{=} \frac{8\pi^3 z_A z_B}{Q^2} \sum_f \mathrm{Tr} \, k_{A,\gamma}^+ \gamma^- H_f^\nu(Q) k_{B,\gamma}^- \gamma^+ \overline{H}_f^\mu(Q)$$

$$\times \int \frac{\mathrm{d}^{2-2\epsilon} b_{\mathrm{T}}}{(2\pi)^{2-2\epsilon}} e^{-i q_{h\mathrm{T}} \cdot b_{\mathrm{T}}} \tilde{S}(b_{\mathrm{T}}) \tilde{D}_{1,\,H_A/f}(z_A, b_{\mathrm{T}}) \tilde{D}_{1,\,H_B/\bar{f}}(z_B, b_{\mathrm{T}})$$

$$+ \text{ polarized terms.} \tag{13.38}$$

13.7 Final version of factorization for $e^+ e^-$ annihilation

After the Fourier transform into transverse coordinate space, the factorization structure in (13.38) has the same multiplicative structure as the Sudakov form factor in Ch. 10. We therefore apply the same manipulations as we used there to obtain an improved scheme for factorization for our process.

One defining property of this scheme is that a square root of the soft factor is absorbed into a redefinition of the TMD fragmentation functions, so no soft factor is needed in the factorization formula itself. This is appropriate, since the non-perturbative part of the soft

factor always appears multiplied by two collinear factors, so that it cannot be independently determined from data.

A second defining property of the scheme is that in the definitions of fragmentation functions, (13.42) below, as many Wilson lines as possible are made light-like. A non-light-like Wilson line appears only in a matrix of a certain elementary soft factor where it is multiplied with a light-like Wilson line. This will have the consequence, just as with the Sudakov form factor, that the evolution equations for the TMD functions are homogeneous. It also makes calculations of integrals simpler.

We will also formulate a further kind of factorization that will determine the TMD functions for small $b_{\rm T}$ in terms of ordinary integrated fragmentation functions. Later, we will add in a correction term to factorization for large $q_{h\,\rm T}/Q$. After that we will have a complete formalism suitable for phenomenological use, with certain functions needing to be obtained by fits to data.

The use of transverse coordinate space simplifies many formulae. An equivalent formalism with transverse momentum variables would involve many convolutions (and their inverses).

The results in Ch. 10 were derived for an abelian gauge theory, and gave definitions for the factors with Wilson lines in certain directions. *In the following treatment, I will only briefly sketch the necessary generalizations of the proofs to extend the results to a non-abelian theory.* The general subtractive method still applies, and the eikonal denominators in the Grammer-Yennie method are the same as before. It is an urgent problem to completely fill in the details of the proofs (problem 13.7).

13.7.1 Definitions of TMD functions

As with the Sudakov form factor in Ch. 10, a basic entity in implementing factorization and subtractions is the bare soft factor defined in (13.23). Its Wilson lines are in non-light-like directions n_A and n_B, whose rapidities are y_A and y_B. They are chosen in the hadron frame as in (10.32). That is, they are space-like (Collins and Metz, 2004), and initially their rapidities approximately correspond to those of the hadrons p_A and p_B. The color charges of the Wilson lines correspond to those of the quark and antiquark. The Fourier transform to transverse coordinate space gives

$$\tilde{S}_{(0)}(b_{\rm T}; y_A, y_B) = \frac{1}{N_c} \langle 0| \ W(\boldsymbol{b}_{\rm T}/2; \infty, n_B)^\dagger_{ca} \ W(\boldsymbol{b}_{\rm T}/2; \infty, n_A)_{ad}$$

$$\times \ W(-\boldsymbol{b}_{\rm T}/2; \infty, n_B)_{bc} \ W(-\boldsymbol{b}_{\rm T}/2; \infty, n_A)^\dagger_{db} \ |0\rangle \Big|_{\text{No SI}}, \qquad (13.39)$$

where Wilson-line self-interactions are again omitted, and the Wilson line rooted at position x is

$$W(x; \infty, n)_{ab} = P \left\{ e^{-ig_0 \int_0^\infty {\rm d}\lambda\, n\cdot A_{(0)\alpha}(x+\lambda n)t_\alpha} \right\}_{ab}. \qquad (13.40)$$

Here the index a corresponds to the start of the line at point x, and the index b corresponds to the end at infinity.

The soft factor has dependence on all parameters of the theory, notably, coupling, masses and renormalization scale, in addition to the parameters indicated explicitly.

In just the same way as we did for the Sudakov form factor, we reorganize the definitions of the factors in the factorization formula, (13.31). After the initial derivation, the collinear factors are matrix elements defined as in the basic formula, (12.35), for a fragmentation function, but with the following modifications:

- In the fragmentation function to hadron H_A, a Wilson line is attached to each of the quark and antiquark fields. Each Wilson line goes to positive infinity in the direction w_B corresponding to the opposite hadron. In the fragmentation function to hadron H_B, the Wilson lines are in direction w_A.
- Wilson-line self-interactions, Fig. 13.4, are omitted.
- Soft subtractions and UV renormalization are applied.

A component of the results is the unsubtracted TMD fragmentation function for hadron H_A:

$$
\tilde{D}_{1,\,H_A/f}^{\text{unsub}}(z_A, b_{\text{T}}, y_{p_A} - y_B)
$$

$$
\overset{\text{def}}{=} \frac{\text{Tr}_{\text{color}}}{N_{c,j}} \frac{\text{Tr}_{\text{Dirac}}}{4} \sum_X \frac{1}{z_A} \int \frac{\mathrm{d}x^-}{2\pi} e^{ik_A^+ x^-} \langle 0|\gamma^+ W(x/2; \infty; n_B)\psi_f(x/2)|p, X, \text{ out}\rangle
$$

$$
\times \langle p, X, \text{ out}|\bar{\psi}_f(-x/2)W(-x/2; \infty; n_B)^{\dagger}|0\rangle\bigg|_{\text{No SI}}
$$

$$
= \frac{\text{Tr}_{\text{color}}}{N_{c,j}} \frac{\text{Tr}_{\text{Dirac}}}{4} \frac{\gamma^+}{z_A} \int \frac{\mathrm{d}k_A^-\, \mathrm{d}^{2-2\epsilon}\boldsymbol{k}_{A\,\text{T}}}{(2\pi)^{4-2\epsilon}} e^{i\boldsymbol{k}_{A\text{T}}\cdot\boldsymbol{b}_{\text{T}}} \xrightarrow{k_A}
$$ (13.41)

where the vector x in the first line is $(0, x^-, \boldsymbol{b}_{\text{T}})$. We do not equip this fragmentation function with a UV-renormalization factor, leaving that to the final definition in (13.42).

Exactly as for the Sudakov form factor, in (10.119a), we combine soft factors into the collinear factors, to make the final definition of the fragmentation function for hadron H_A:

$$
\tilde{D}_{1,\,H_A/f}(z_A, b_{\text{T}}; \zeta_A; \mu)
$$

$$
\overset{\text{def}}{=} \lim_{\substack{y_A \to +\infty \\ y_B \to -\infty}} \tilde{D}_{1,\,H_A/f}^{\text{unsub}}(z_A, b_{\text{T}}; y_{p_A} - y_B) \sqrt{\frac{\tilde{S}_{(0)}(b_{\text{T}}; y_A, y_n)}{\tilde{S}_{(0)}(b_{\text{T}}; y_A, y_B)\, \tilde{S}_{(0)}(b_{\text{T}}; y_n, y_B)}}
$$

$$
\times \text{ UV-renormalization factor}
$$

$$
= \tilde{D}_{1,\,H_A/f}^{\text{unsub}}(z_A, b_{\text{T}}; y_{p_A} - (-\infty)) \sqrt{\frac{\tilde{S}_{(0)}(b_{\text{T}}; +\infty, y_n)}{\tilde{S}_{(0)}(b_{\text{T}}; +\infty, -\infty)\, \tilde{S}_{(0)}(b_{\text{T}}; y_n, -\infty)}}\, Z_D Z_2.
$$

$$
(13.42)
$$

As in (10.119a), y_n is an arbitrary rapidity value, used to specify non-light-like Wilson lines. It will have the function in the factorization formula of separating left- and right-moving quanta. We use the notation with infinite-rapidity Wilson lines to imply the appropriate limit operations. The fragmentation function depends on the rapidity difference $y_{p_A} - y_n$. But for the corresponding argument of the fragmentation function we use the following variable:

$$\zeta_A \stackrel{\text{def}}{=} 2(k_{A,h}^+)^2 e^{-2y_n} = \frac{2(p_{A,h}^+)^2 e^{-2y_n}}{z_A^2} = \frac{m_A^2}{z_A^2} e^{2(y_{p_A} - y_n)}. \tag{13.43}$$

This is a convenient variable for use in renormalization. Compare (10.127a).

As explained following (10.119a), UV renormalization and removal of the UV regulator (i.e., space-time dimension $n \to 4$) are to be applied *after* taking the limits of infinite rapidity for the Wilson lines. In the case of the integrated fragmentation function there was an integral over all external parton transverse momentum, and the associated UV divergence gave a non-trivial RG equation of the DGLAP type. But for the TMD function, this integral is absent, and UV divergences are only in virtual corrections, essentially the same as in the collinear factors for the Sudakov form factor. Since $\tilde{D}^{\text{unsub}}$ is defined with renormalized quark fields, the multiplicative UV-renormalization factor in (13.42) is written as $Z_D Z_2$, where Z_2 is the wave-function renormalization factor of the quark field. Then Z_D is the ratio of the renormalized fragmentation function to the unrenormalized fragmentation function defined with *bare* fields. The anomalous dimension will be obtained from Z_D.

A fragmentation function for the other hadron is defined like (13.42), just with the roles of the plus and minus coordinates exchanged, and with exchange of the labels A and B. Instead of ζ_A we use

$$\zeta_B \stackrel{\text{def}}{=} 2(k_{B,h}^-)^2 e^{2y_n} = \frac{2(p_{B,h}^-)^2 e^{2y_n}}{z_B^2} = \frac{m_B^2}{z_B^2} e^{2(y_n - y_{p_B})}. \tag{13.44}$$

Note that with the values of $k_{A,h}^+$ and $k_{B,h}^-$ specified in Sec. 13.3.2, and with neglect of power-suppressed corrections, we have

$$\zeta_A \zeta_B = \frac{Q^4}{\cos^4(\delta\theta/2)} \quad \text{(original values).} \tag{13.45}$$

But we will be able to clean up the factorization formula by changing the values of ζ_A and ζ_B slightly.

13.7.2 Wilson-line self-interactions in final definitions

For the same reasons as for the soft factor, Wilson-line self-interactions were omitted from the definition of the unsubtracted fragmentation function, (13.41). We now show that in the final definition of the complete fragmentation function, (13.42), we can replace the unsubtracted collinear and soft factors by versions with Wilson-line self-interactions allowed.

In an abelian theory, Wilson-line self-interactions just gave an overall factor, e.g., in (10.89). Thus it was straightforward to show that the self-interactions cancel in the

combinations relevant to (10.119). Thus we could retain Wilson-line self-energies on the r.h.s. of this equation, and obtain gauge independence.

For the non-abelian case, the steps are not so direct. This is because we can no longer use (10.100) to disentangle the different gluons attaching to a Wilson line. Instead we use a factorization theorem for each of the factors on the r.h.s. of (13.42), in the limit that $y_A \to \infty$ and $y_B \to -\infty$; cf. Sec. 10.8.7. Each factor then becomes the product of a hard factor, a soft factor, and two collinear factors. For each Wilson line in (13.42), we obtain a particular collinear factor after this new factorization, and it is these collinear factors that we treat as the Wilson-line self-interactions.

To see that the Wilson-line self-interactions cancel in (13.42), we simply count the number of appearances of each kind of self-interaction factor in the complete expression. For example, the Wilson-line self-interaction factor for the y_B Wilson line of D^{unsub} is canceled by the two y_B Wilson-line self-interaction factors from the two factors of $\tilde{S}$ in the denominator of the square-root factor.

The factorization of Wilson-line self-interaction contributions is correct for each correlation function up to errors suppressed by exponentials of the differences in Wilson-line rapidities, e.g., $e^{-(y_A - y_B)}$. Thus, when the infinite rapidity limits are taken in (13.42), these errors become exactly zero. The result for the abelian Sudakov form factor is just a special case.

An immediate and important advantage is that the collinear factors defined in (13.42) are gauge invariant. Hence the results of calculations are independent of the choice of gauge fixing, unlike the case for the individual factors on the r.h.s. of (13.42); see problem 10.9.

It is true that the Wilson lines do not quite join at infinity. For example, in (13.39) we have segments at different transverse positions. To get an exactly gauge-invariant operator, two links must be inserted at infinity in a transverse direction. But the factorization argument for cancellation of Wilson-line self-interactions also applies to the transverse links at infinity.

13.7.3 Factorization

To complete the factorization formula with the redefined fragmentation functions, we anticipate a result from Sec. 13.12 below that gives an additive correction term Y to the structure derived so far. Our derivation has been appropriate for small $q_{h\,\mathrm{T}}$: we have neglected not only terms suppressed by a power of a hadronic mass divided by Q, but also terms suppressed by a power of $q_{h\,\mathrm{T}}/Q$. But when $q_{h\,\mathrm{T}}$ is of order Q, conventional factorization with integrated fragmentation functions is valid. So in Sec. 13.12, we will show how to formulate a large-$q_{h\,\mathrm{T}}$ correction term Y. The resulting factorization formula is

$$
W^{\mu\nu} = \frac{8\pi^3 z_A z_B}{Q^2} \sum_f \mathrm{Tr}\, k_{A,\gamma}^+ \gamma^-\, H_f^\nu(Q)\, k_{B,\gamma}^- \gamma^+\, \overline{H}_f^\mu(Q)
$$

$$
\times \int \frac{\mathrm{d}^{2-2\epsilon} \boldsymbol{b}_\mathrm{T}}{(2\pi)^{2-2\epsilon}} e^{-i\boldsymbol{q}_{h\,\mathrm{T}} \cdot \boldsymbol{b}_\mathrm{T}}\, \tilde{D}_{1,\,H_A/f}(z_A, b_\mathrm{T}; Q^2 e^{-2y_n})\, \tilde{D}_{1,\,H_B/\bar{f}}(z_B, b_\mathrm{T}; Q^2 e^{2y_n})
$$

$$
+ \text{polarized terms} + \text{large-}q_{h\,\mathrm{T}}\ \text{correction}, Y. \tag{13.46}
$$

As in earlier factorization formulae, we use "polarized terms" to indicate term(s) that involve the entangled transverse-spin state. The values of the ζ_A and ζ_B arguments of the fragmentation functions are changed from the values in (13.43) and (13.44), thereby removing the $\cos(\delta\theta/2)$ in (13.45). This will simplify the formulae used in phenomenology. Since the effect is of order $q_{h\,T}^2/Q^2$, it is comparable to errors in the approximants used in the derivation, and does not affect the correctness of the formula. A correct Y term will cancel $q_{h\,T}^2/Q^2$ errors in the TMD term, including those associated with the changes of the values of ζ_A and ζ_B to those in (13.46). Hence the overall result for $W^{\mu\nu}$ is valid for all $q_{h\,T}$, small and large, with relative errors suppressed by a power of mass divided by Q.

In the TMD part of this and previous formulae, the collinear, soft and hard factors appear in the same way as in the Sudakov form factor in Ch. 10. In particular, a soft factor is absent in the final formula. The changes relative to Ch. 10 simply accommodate that the factors correspond to scattering amplitudes times conjugate amplitudes and that the Wilson lines etc. are shifted transversely between the amplitude and the conjugate. The collinear factors have the operators and normalizations appropriate for fragmentation; the Dirac structure is unchanged from a non-gauge theory. Relative to the definitions in a non-gauge theory, only the Wilson-line factors are new.

13.8 Evolution equations for TMD fragmentation functions

When initially conceived, a TMD fragmentation function was simply the number density of hadrons in a parton-induced jet. With its complete definition, it acquires dependence on both a renormalization scale and on ζ. We can regard this dependence as the effect of recoil against emission of soft gluons into approximately a range determined by μ and ζ. Appropriate values of these parameters are energy dependent.

To regain predictive power and effective universality together with some extra predictions, we now derive evolution equations: an RG equation for the μ dependence and a Collins-Soper (CS) equation for the rapidity dependence. The overall structure is the same as for the Sudakov form factor.

13.8.1 CS evolution of TMD fragmentation function

The CS equation has the form

$$\frac{\partial \ln \tilde{D}_{1,\,H_A/f}(z_A, b_{\mathrm{T}}; \zeta_A, \ldots)}{\partial \ln \sqrt{\zeta_A}} = \tilde{K}(b_{\mathrm{T}}; \mu). \tag{13.47}$$

The derivative is equivalent to a derivative with respect to $-y_n$. Since the only dependence on y_n is in the S factors in (13.42), we have

$$\tilde{K}(b_{\mathrm{T}}; \ldots) = \frac{\partial}{\partial y_n}\left[\frac{1}{2}\ln\tilde{S}_{(0)}(b_{\mathrm{T}}; y_n, -\infty) - \frac{1}{2}\ln\tilde{S}_{(0)}(b_{\mathrm{T}}; +\infty, y_n)\right] + \text{UV counterterm}$$

$$= \frac{1}{2\tilde{S}_{(0)}(b_{\mathrm{T}}; y_n, -\infty)}\frac{\partial\tilde{S}_{(0)}(b_{\mathrm{T}}; y_n, -\infty)}{\partial y_n}$$

$$- \frac{1}{2\tilde{S}_{(0)}(b_{\mathrm{T}}; +\infty, y_n)}\frac{\partial\tilde{S}_{(0)}(b_{\mathrm{T}}; +\infty, y_n)}{\partial y_n} + \text{UV c.t.} \tag{13.48}$$

This is normalized to be like K in Ch. 10. Since K is derived from the soft factor, it is the same for all quark and antiquark fragmentation functions. It would be different for the fragmentation of a gluon, which is a color octet.

Now in a differentiated soft factor, e.g., $\partial S(b_{\mathrm{T}}, y_A, y_B)/\partial y_A$, there is a sum of terms in each of which one Wilson-line vertex and its neighboring line are differentiated with respect to rapidity. The resulting vertex is the same as in Fig. 10.27 for the Sudakov form factor, but with the insertion of the appropriate color matrix. Exactly as for the Sudakov form factor, the momentum at the differentiated vertex is, to leading power, close in rapidity to that of the parent Wilson line. Factorization then gives the original soft factor times a factor associated with differentiated vertex. Taking the rapidity difference of the Wilson lines to infinity then removes the power-suppressed corrections to factorization, and leaves a kernel $\tilde{K}$ that depends on b_{T} and on the parameters of the theory (μ, $g(\mu)$, etc.), but not on the Wilson-line rapidities.

13.8.2 RG evolution of K

As with the Sudakov form factor, the evolution kernel $\tilde{K}$ is renormalized by adding a counterterm, and this gives an additive anomalous dimension. The UV divergence only arises from virtual graphs, so it has no b_{T} dependence. The RG equation for $\tilde{K}$ then has the form

$$\frac{\mathrm{d}\tilde{K}}{\mathrm{d}\ln\mu} = -\gamma_K(g(\mu))\,. \tag{13.49}$$

13.8.3 RG evolution of TMD fragmentation function

Since the UV divergences of the TMD fragmentation function $\tilde{D}$ arise only from virtual graphs, the associated RG equation arises from the overall Z_D factor in (13.42). Thus the RG equation for $\tilde{D}$ has the form

$$\frac{\mathrm{d}\ln\tilde{D}_{1,\,H_A/f}(z_A, b_{\mathrm{T}}; \zeta_A, \ldots)}{\mathrm{d}\ln\mu} = \gamma_D\big(g(\mu); \zeta_A/\mu^2\big)\,. \tag{13.50}$$

Unlike the DGLAP equation, there is no convolution with the longitudinal momentum fraction z_A. However, as with the Sudakov form factor (see Sec. 10.11.4) the anomalous dimension does depend on the longitudinal momentum of the quark, via the variable ζ_A defined in (13.43).

We obtain the energy dependence of γ_D, by the same proof as for the Sudakov form factor in Sec. 10.11.4, and obtain

$$\gamma_D\big(g(\mu); \zeta_A/\mu^2\big) = \gamma_D(g(\mu); 1) - \frac{1}{2}\gamma_K(g(\mu))\ln\frac{\zeta_A}{\mu^2}\,. \tag{13.51}$$

13.9 Flavor dependence of CS and RG evolution

In the most common applications, TMD fragmentation functions (and also TMD parton densities) are used only for Dirac quarks. But TMD functions can be defined for any kind of
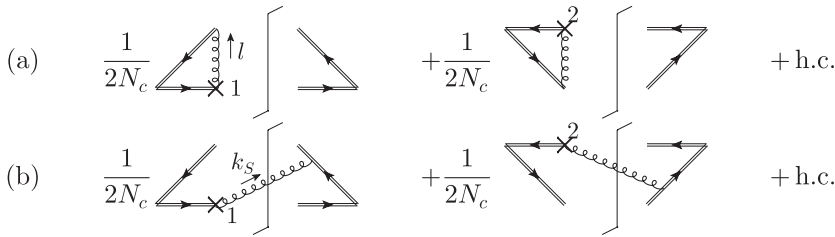
Fig. 13.5. Lowest-order graphs for K: (a) virtual gluon, (b) real gluon. Note the addition of the hermitian conjugate (h.c.) graphs, where the differentiated vertex is on the opposite side of the final-state cut. The empty Wilson lines on the right in the virtual graphs give a unit factor for zeroth-order Wilson lines. The overall factor of $1/N_c$ is from (13.39), and the factor of $\frac{1}{2}$ is from (13.48).

parton, both for the gluon in QCD and for other partonic fields in hypothesized extensions of QCD.

The kernel K and its anomalous dimension γ_K arise from the Wilson-line soft factors, and thus depend only on the color representation of the parton. Thus there are separate versions of these for the gluon, which we could denote K_8 and γ_{K8}. The lowest-order values are obtained from those for ordinary quarks by changing C_F to C_A.

But in a supersymmetric extension of QCD, we would not need any extra functions. The extra fields in such a theory are squarks and gluinos. A squark is a scalar triplet, so it would use the same values of K and γ_K as ordinary quarks. This applies both to the perturbative and non-perturbative parts, of course. A gluino is a spin-$\frac{1}{2}$ octet, so it would need the same K_8 and γ_{K8} as a gluon.

In contrast, the anomalous dimension γ_D would differ between all these types of parton.

13.10 Analysis of CS kernel K: perturbative and non-perturbative

13.10.1 Feynman rules for K

The definition of K in (13.48) involves differentiation of Wilson lines in $\tilde{S}$ with respect to rapidity. The basic vertex needed for the derivatives are obtained from differentiating one Wilson-line vertex and its neighboring line, exactly as in Fig. 10.27, but with an appropriate color matrix.

At lowest order, the resulting graphs are shown in Fig. 13.5, a simple generalization of those for the Sudakov form factor.

In QCD, we no longer have the simplification that we had in an abelian theory where each Wilson line is a graphical exponential of its first-order term. Therefore higher-order graphs for K are more complicated than the simple connected graphs shown in Fig. 10.23 for the abelian theory. It is left as a research exercise to search for any corresponding simplification in a non-abelian theory.

13.10.2 LO calculation of K

LO virtual graphs for K

In (10.134), we calculated K for the Sudakov form factor. For the *virtual* graphs in the present context, Fig. 13.5(a), almost the same calculation applies. The factors of $\frac{1}{2}$ in the definition of K for fragmentation are now canceled by the addition of hermitian conjugate graphs. For QCD, we insert the usual QCD color factor of C_F, and we make the gluon massless.

In momentum space, there is no final-state momentum for the virtual graphs, so for the contribution of these graphs in (13.23) we insert a factor $(2\pi)^{4-2\epsilon}\delta^{(4-2\epsilon)}(k_S)$. After the integration given in (13.23), we have a factor $\delta^{(2-2\epsilon)}(\boldsymbol{k}_{\mathrm{T}})$ relative to the Sudakov form factor case. The Fourier transform to transverse coordinate space converts this to unity, to give

$$\tilde{K}_{1V} = \frac{-g^2 C_F (4\pi\mu^2)^\epsilon}{4\pi^3} \int \mathrm{d}^{2-2\epsilon} l_{\mathrm{T}} \frac{1}{l_{\mathrm{T}}^2} + \frac{g^2 C_F S_\epsilon}{4\pi^2\epsilon}. \tag{13.52}$$

Here, the UV counterterm is in the $\overline{\mathrm{MS}}$ scheme, and the $\boldsymbol{l}_{\mathrm{T}}$ integral is left explicit. This exhibits a negative IR divergence at $\boldsymbol{l}_{\mathrm{T}} = 0$, which will cancel against a positive divergence from the real emission graphs. The subscript "$1V$" denotes "1-loop virtual".

LO real graphs for K

In Feynman gauge, each of the two graphs in Fig. 13.5(b) gives an equal result, as do their hermitian conjugates; this is checked by explicit calculation. So the complete result is given by multiplying one graph (including its explicit factor of $\frac{1}{2}$) by 4. With the rule in Fig. 10.27 for the differentiated line, we get

$$\begin{aligned}
\tilde{K}_{1R} &= \frac{-4g^2 C_F \mu^{2\epsilon}}{(2\pi)^{4-2\epsilon}} \int \mathrm{d}^{4-2\epsilon} k_S \, e^{ik_{S\mathrm{T}}\cdot\boldsymbol{b}_{\mathrm{T}}} \frac{(2\pi)\delta(k_S^2)\theta(k_S^0)}{(k_S^- e^{y_n} - k_S^+ e^{-y_n} + i0)^2} \\
&= \frac{g^2 C_F (4\pi^2\mu^2)^\epsilon}{4\pi^3} \int \mathrm{d}^{2-2\epsilon} \boldsymbol{k}_{\mathrm{T}} \frac{e^{i\boldsymbol{k}_{\mathrm{T}}\cdot\boldsymbol{b}_{\mathrm{T}}}}{k_{\mathrm{T}}^2}.
\end{aligned} \tag{13.53}$$

LO total for K

The IR divergence at zero transverse momentum cancels between the real and virtual graphs:

$$\tilde{K}_1 = \frac{g^2 C_F (4\pi^2\mu^2)^\epsilon}{4\pi^3} \int \mathrm{d}^{2-2\epsilon} \boldsymbol{k}_{\mathrm{T}} \frac{e^{i\boldsymbol{k}_{\mathrm{T}}\cdot\boldsymbol{b}_{\mathrm{T}}} - 1}{k_{\mathrm{T}}^2} + \frac{g^2 C_F S_\epsilon}{4\pi^2\epsilon}. \tag{13.54}$$

To perform the $\boldsymbol{k}_{\mathrm{T}}$ integral, we use (A.45), and get

$$\tilde{K}_1 = \frac{g^2 C_F}{4\pi^2} \left[(\pi\mu^2 b_{\mathrm{T}}^2)^\epsilon \Gamma(-\epsilon) + \frac{S_\epsilon}{\epsilon} \right] \overset{\epsilon=0}{=} -\frac{g^2 C_F}{4\pi^2} \left[\ln(\mu^2 b_{\mathrm{T}}^2) - \ln 4 + 2\gamma_E \right]. \tag{13.55}$$

The anomalous dimension, from (13.49), is therefore

$$\gamma_K = \frac{g^2 C_F}{2\pi^2} + O(g^4). \tag{13.56}$$

13.10.3 Analysis of b_T dependence for K

The $\boldsymbol{b}_T$ dependence of TMD functions and of $\tilde{K}$ determines the transverse-momentum dependence of cross section, and so it is important to understand to what extent the $\boldsymbol{b}_T$ dependence can be predicted by perturbative calculations.

At large $\boldsymbol{b}_T$ the dependence is non-perturbative, simply because the operators are separated by a large distance. There the functions must be obtained by analyzing experimental data, given the present lack of non-perturbative calculations. In contrast, at small $\boldsymbol{b}_T$ we can employ perturbative methods, as we will now see. Since the boundary between non-perturbative and perturbative regions is quite vague, we will also need a method to combine for a single function perturbative predictions and non-perturbative fits.

Now in the definition of the soft factor $\tilde{S}(b_T)$, there is an integral over the external momentum k_S, with the Fourier-transform factor $e^{i\boldsymbol{k}_{ST}\cdot\boldsymbol{b}_T}$ providing, roughly speaking, an upper cutoff at $k_{ST} \sim 1/b_T$. We have the same situation as in the e^+e^- annihilation cross section that this gives an IR-safe quantity. The same applies to $\tilde{K}$, which is a derivative of $\tilde{S}$, as is evidenced by the canceled IR singularity in (13.54).

So to calculate $\tilde{K}(b_T)$ at small b_T we simply apply an RG transformation to set μ of order $1/b_T$:

$$\tilde{K}(b_T; \mu, g(\mu), m(\mu)) \simeq \tilde{K}\left(b_T; \frac{C_1}{b_T}, g\left(\frac{C_1}{b_T}\right), 0\right) - \int_{C_1/b_T}^{\mu} \frac{d\mu'}{\mu'} \gamma_K\big(g(\mu')\big). \quad (13.57)$$

On the r.h.s., K has its renormalization mass proportional to $1/b_T$, which eliminates large logarithms. The constant of proportionality, C_1, can be used to optimize the accuracy of perturbative calculations. In the $\overline{\text{MS}}$ scheme, a value not far from unity is appropriate. Then, for example, truncating perturbation theory for $\tilde{K}$ to the first-order term gives an error of order the first term omitted, i.e., $O(g^4)$. We have also chosen to neglect quark masses relative to $1/b_T$, as is appropriate for light quarks.

In applications, we will set μ equal to the value used in calculating the hard scattering perturbatively, i.e., of order Q, unambiguously in a perturbative domain. As b_T is varied with μ fixed, the largest contribution to the r.h.s. of (13.57) comes from the integral over the anomalous dimension.

Evidently the accuracy of a perturbative estimate worsens as b_T increases, and for large enough b_T, presumably around 0.5 fm, perturbation theory becomes inapplicable. In this case, we can perform a transformation to a value μ_0 of the renormalization mass μ_0 that stays fixed when we change the experimental energy Q and hence change μ. Thus we write

$$\tilde{K}(b_T; \mu, g(\mu), m(\mu)) = \tilde{K}(b_T; \mu_0, g(\mu_0), m(\mu_0)) - \int_{\mu_0}^{\mu} \frac{d\mu'}{\mu'} \gamma_K(g(\mu')). \quad (13.58)$$

This demonstrates an important result: the non-perturbative information in K is contained in a single universal function of b_T. (The universality is between all processes using TMD functions for color-triplet partons.) As we will see, this function can be measured from the derivative with respect to energy of a suitable cross section. In principle, the derivative

can be taken at one energy, thereby allowing a prediction of the cross section at other energies.

<p style="text-align:center">Consequences in transverse-momentum space</p>

When we Fourier-transform back to transverse momentum, perturbative calculations at small b_T conveniently combine two types of perturbatively calculable information. First, the singularity of $\tilde{K}(b_T)$ at small b_T determines the shape of $K(k_T)$ at large k_T. Second, the value of $\tilde{K}$ at small b_T determines the integral of $K(k_T)$ over all k_T up to about $1/b_T$. Similar remarks apply to the TMD fragmentation function.

13.10.4 Matching perturbative and non-perturbative b_T dependence

To combine information on $\boldsymbol{b}_T$ dependence from perturbative calculations valid at small enough $\boldsymbol{b}_T$ with a non-perturbative part that must be determined by a fit to experimental data, a matching procedure was formulated by Collins and Soper (1982a). First a parameter b_{max} is chosen which has the interpretation of the maximum distance at which perturbation theory is to be trusted. One value (Landry *et al.*, 2003) that has been used is $b_{max} = 0.5\,\mathrm{GeV}^{-1} = 0.1\,\mathrm{fm}$.

Then a function $\boldsymbol{b}_*(\boldsymbol{b}_T)$ is defined with the properties that at small $\boldsymbol{b}_T$ it is the same as $\boldsymbol{b}_T$, and that at large $\boldsymbol{b}_T$ it is no larger than b_{max}. The standard choice is

$$\boldsymbol{b}_* \overset{\text{def}}{=} \frac{\boldsymbol{b}_T}{\sqrt{1 + b_T^2/b_{max}^2}}. \tag{13.59}$$

Changes in the form of this function or in the value of b_{max} do not affect the physical cross section, but only the way in which non-perturbative phenomena are parameterized.

We now write $\tilde{K}(b_T) = \tilde{K}(b_*) + $ correction term. The idea is that $\tilde{K}(b_*)$ is always in a situation where perturbation theory is appropriate, and the correction term is only important at large $\boldsymbol{b}_T$. Therefore we write

$$
\begin{aligned}
\tilde{K}(b_T; \mu, \ldots) &= \tilde{K}(b_*; \mu, g(\mu), m(\mu)) \\
&\quad + \big[\tilde{K}(b_T; \mu, g(\mu), m(\mu)) - \tilde{K}(b_*; \mu, g(\mu), m(\mu))\big] \\
&= \tilde{K}(b_*; C_1/b_*, g(C_1/b_*), 0) - \int_{C_1/b_*}^{\mu} \frac{\mathrm{d}\mu'}{\mu'} \gamma_K(g(\mu')) \\
&\quad + \big[\tilde{K}(b_T; \mu_0, g(\mu_0), m(\mu_0)) - \tilde{K}(b_*; \mu_0, g(\mu_0), m(\mu_0))\big] \\
&= \tilde{K}(b_*; C_1/b_*, g(C_1/b_*), 0) - \int_{C_1/b_*}^{\mu} \frac{\mathrm{d}\mu'}{\mu'} \gamma_K(g(\mu')) - g_K(b_T), \quad (13.60)
\end{aligned}
$$

where the correction term is denoted $-g_K$. Phenomenologically it is a function of one variable b_T, to be fit to data. It is RG invariant, since it is a difference of $\tilde{K}$ at two values of its position argument. The correction term vanishes as $\boldsymbol{b}_T \to 0$. Recent fits use a quadratic

ansatz:

$$g_K(b_T) = \frac{1}{2} g_2 b_T^2. \tag{13.61}$$

The measured value of g_2 is correlated with the value of b_{max}, and with assumptions about other non-perturbative functions; see Sec. 14.5.3. Landry *et al.* (2003) and Konychev and Nadolsky (2006) found

$$g_2 = \begin{cases} 0.68\,^{+0.01}_{-0.02}\,\text{GeV}^2 & \text{with } b_{max} = 0.5\,\text{GeV}^{-1}, \\ 0.17 \pm 0.02\,\text{GeV}^2 & \text{with } b_{max} = 1\,\text{GeV}^{-1}. \end{cases} \tag{13.62}$$

(The second number is my average of two fits.) Then

$$g_K(b_T) \simeq \begin{cases} 0.34\, b_T^2 & \text{with } b_{max} = 0.5\,\text{GeV}^{-1}, \\ 0.08\, b_T^2 & \text{with } b_{max} = 1\,\text{GeV}^{-1}. \end{cases} \tag{13.63}$$

The fits are made with truncated perturbative approximations for both $\tilde{K}(b_*; C_1/b_*, g(C_1/b_*), 0)$ and $\gamma_K(g(\mu'))$. Because the coupling increases with decreasing scale, the approximations lose accuracy when applied at larger values of b_* compared with lower values. A phenomenological fit for the function $g_K(b_T)$ in (13.60) effectively includes an allowance for errors in truncated perturbation theory for scales near b_{max}.

Thus one should *not* expect the numerical values of $g_K(b_T)$ to be stable against the inclusion of yet higher-order perturbative estimates of $\tilde{K}$ and γ_K. Only the total value of $\tilde{K}(b_T)$ should be stable against improvements in perturbative calculations.

Note that the numerical results quoted from Landry *et al.* (2003) were from fits to Drell-Yan data. In describing them here for their application to e^+e^- annihilation, we are using a result to be explained later that the soft function is the same in the two reactions.

13.11 Relation of TMD to integrated fragmentation function

We now generalize the methods of Secs. 13.10.3 and 13.10.4 to analyze the dependence of the fragmentation function on b_T, and to formulate perturbative and non-perturbative parts.

13.11.1 Perturbative small-b_T dependence

First, we analyze the small-b_T region. We show that in contrast to the case of the evolution kernel K, the perturbative calculation for a TMD fragmentation function at small b_T does not determine the fragmentation function absolutely, but only expresses it, by a factorization property, in terms of a perturbative coefficient convoluted with integrated fragmentation functions. The integrated fragmentation functions themselves must still be obtained from experiment. This result does give notable predictive power since a function of two kinematic variables is expressed in terms of a non-perturbative function of one variable.
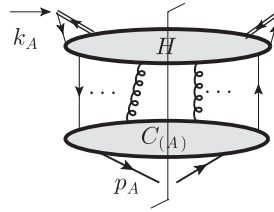
Fig. 13.6. Leading regions for TMD fragmentation function at small $\boldsymbol{b}_{\mathrm{T}}$.

See Sec. 13.11.2 for how to combine this with non-perturbative information for large b_{T}.

To motivate that a relation should exist between a TMD fragmentation function at small b_{T} and an integrated fragmentation function, we recall the discussion at the beginning of Sec. 13.6. There we showed that in super-renormalizable non-gauge model theories, a TMD fragmentation function at zero b_{T} equals the corresponding integrated fragmentation function (up to a standard normalization factor); this is the parton-model result. In QCD, this relation fails, because of the need to renormalize fragmentation functions and because of complications associated with the soft factors in (13.42).

I will now formulate a corrected relation. It is a factorization formula involving a coefficient function whose lowest-order value is unity, corresponding to the parton-model result.

Region analysis

We start with a region analysis for the unsubtracted unintegrated TMD fragmentation function (13.41). Leading regions involve hard, collinear and soft subgraphs. The soft subgraphs connect the collinear subgraphs, and there are collinear factors associated with the detected hadron and with the Wilson line. The hard factor is associated with the external quark–Wilson-line vertices. Its lowest-order term is just these vertices. There can be higher-order hard subgraphs with highly virtual loops, and there can be further hard subgraphs with production of final-state jets of high transverse momentum, the transverse momenta being limited basically by the large value of $1/b_{\mathrm{T}}$. The structure is essentially the same as we encountered for simple inclusive cross sections in $e^{+}e^{-}$ annihilation, around Fig. 12.4. As in that case, the sum/integral over final states in each extra jet is fully inclusive, so after a sum-over-cuts, as in Sec. 12.8.7, the subgraphs for the extra high-transverse-momentum jets are effectively far off-shell and count as part of the hard part.

But now a difference arises, that the definition of the subtracted TMD fragmentation function (13.42) includes subtractions to remove the opposite (p_B-associated) collinear region and the soft region. So the only remaining effective regions have a subgraph collinear to p_A and a possible hard subgraph, as shown in Fig. 13.6. The parton-model result applies when the only hard subgraphs are trivial, i.e., when all the parton lines in the graph on the last line of (13.41) are hadron-collinear.

Factorization for TMD at small b_T

We now apply the usual factorization argument to Fig. 13.6, summed over all cases and with double-counting subtractions. The extra gluons entering the hard part are converted to Wilson lines by Ward identities. Since the integration over transverse momenta in the collinear part is limited solely by $1/b_T$ in the hard part, the collinear factor gives an *integrated* fragmentation function. We get

$$\tilde{D}_{1,\,H_A/f}(z_A, b_T; \zeta_A; \mu)$$
$$= \sum_j \int_{z_A}^1 \frac{d\hat{z}}{\hat{z}^{3-2\epsilon}}\, d_{H_A/j}(\hat{z}; \mu)\, \tilde{C}_{j/f}(z_A/\hat{z}, b_T; \zeta_A, \mu, g(\mu)) + O[(mb_T)^p]. \quad (13.64)$$

The error term is suppressed by some power of transverse position. The sum over j is over all types of parton, including gluons and antiquarks. The coefficient function $\tilde{C}_{f/j}$ is calculated, as usual for a hard factor, from graphs with external on-shell parton of type j, with double-counting subtractions that cancel all collinear contributions.

Since the on-shell parton has infinite rapidity, we convert the dependence on the rapidity y_n to a dependence of C on an energy variable ζ_A, defined by (13.43). The lowest-order coefficient is

$$\tilde{C}_{j/f}(z_A/\hat{z}, b_T; \zeta_A, \mu, g(\mu)) = \delta_{jf}\delta(z_A/\hat{z} - 1) + O(g^2). \quad (13.65)$$

The integral in (13.64) has a measure $d\hat{z}/\hat{z}^{3-2\epsilon}$, rather than the $d\hat{z}/\hat{z}$ that we would get for a corresponding formula with a parton density. This arises from the different powers of z in the normalizations of the definitions of the TMD and integrated fragmentation function, (12.39) and (12.40). Although the formula is phenomenologically applied at $\epsilon = 0$, it was written for a general ϵ. This allows the factorization formula also to be applied in perturbative calculations, where intermediate stages use dimensional regularization.

Logarithms in coefficient

Evolution equations for the coefficient can be derived from the CS and RG evolution equations for the TMD fragmentation function and the DGLAP equation for the integrated fragmentation function. They show that the dependence of the coefficient on μ and on ζ_A is logarithmic in each order of perturbation theory. Hence by dimensional analysis the dependence on b_T is also logarithmic. Thus the functional form of the b_T dependence in each order of perturbation theory is a polynomial in $\ln b_T^2$. From the evolution equations it can be seen that the order of the polynomial is $2L$ where L is the number of loops: i.e., there are two logarithms per loop, giving leading logarithms characteristic of the Sudakov form factor. Fourier transformation gives $1/k_T^2$ times a polynomial in $\ln k_T^2$, and the order of this polynomial is $2L - 1$.

NLO calculations

To see how actual calculations work and for the values of the coefficients, see Sec. 13.14.

TMD fragmentation function at large k_T

Fourier transformation of (13.64) gives factorization for the TMD fragmentation function at large transverse momentum:

$$D_{1,\,H_A/f}(z_A, k_T; \zeta_A; \mu)$$

$$= \sum_j \int_{z_A}^1 \frac{\mathrm{d}\hat{z}}{\hat{z}^{3-2\epsilon}} \, d_{H_A/j}(\hat{z}; \mu) \; C_{j/f}\left(\frac{z_A}{\hat{z}}, k_T; \zeta_A, \mu, g(\mu)\right) + O\left[\left(\frac{m}{k_T}\right)^p \frac{1}{k_T^2}\right]. \quad (13.66)$$

13.11.2 Matching perturbative and non-perturbative b_T dependence for TMD fragmentation

To combine the perturbative information on fragmentation at small b_T with non-perturbative information (to be fitted to data) at large b_T, we copy the method applied in Sec. 13.10.4 to the kernel K.

Intrinsic transverse momentum dependence and energy dependence

A complication is that in addition to the kinematic variables z and $\boldsymbol{b}_T$, the TMD fragmentation function depends on two parameters $y_{p_A} - y_n$ and μ, which can be thought of as cutoffs on internal gluon momenta. The CS and RG equations control dependence on these parameters. In an application, we will normally set μ of order the large kinematic variable Q, to allow a useful perturbative calculation of the hard scattering; we might choose y_n to be zero in the overall CM frame. Thus the values of $y_{p_A} - y_n$ and μ change, depending on the kinematics of the process being considered.

So we solve the evolution equations to gives the TMD fragmentation function in terms of its value at fixed reference values of ζ_A and μ:

$$\tilde{D}_{1,\,H_A/f}(z_A, b_T; \zeta_A; \mu) = \tilde{D}_{1,\,H_A/f}\left(z_A, b_T; m_A^2/z_A^2; \mu_0\right) \exp\left\{ \ln \frac{\sqrt{\zeta_A} z_A}{m_A} \tilde{K}(b_T; \mu_0) \right.$$

$$\left. + \int_{\mu_0}^\mu \frac{\mathrm{d}\mu'}{\mu'} \left[\gamma_D\big(g(\mu'); 1\big) - \ln \frac{\sqrt{\zeta_A}}{\mu'} \gamma_K\big(g(\mu')\big) \right] \right\}. \quad (13.67)$$

Here, the reference value of ζ_A was chosen to correspond to $y_{p_A} = y_n$. Some other value could equally well be used, but this value is appropriate as the limit of where the detected hadron is moving to the right in the rest frame of the vector n. As for the reference value μ_0 of the renormalization scale, it should be in the perturbative region, so that low-order perturbative calculations of γ_D and γ_K are useful. Notice that the μ dependence gives an overall normalization change, but does not affect the shape of the b_T dependence of the fragmentation function.

The dependence on ζ_A involves the function $\tilde{K}(b_T)$, so it gives energy dependence to the shape of the transverse momentum distribution. We characterize the result as follows. The

function $\tilde{D}$ at its reference value of the parameters can be thought of as the Fourier transform of an intrinsic transverse momentum distribution of a hadron in its parent parton, essentially a parton-model concept. But this is multiplied by $e^{\ln(\sqrt{\zeta_A}z_A/m_A)\tilde{K}(b_{\mathrm{T}};\mu_0)}$. This is the effect of energy-dependent recoil against the emission of soft gluons. In momentum space we can treat its effects as the result of convoluting the intrinsic distribution with $\ln(\sqrt{\zeta_A}z_A/m_A)$ factors of the Fourier transformation of $e^{\tilde{K}(b_{\mathrm{T}};\mu_0)}$. Thus we can treat $e^{\tilde{K}(b_{\mathrm{T}};\mu_0)}$ as giving the distribution of gluon emission per unit rapidity, with the emission being uniform in rapidity. Note that perturbative calculations and fits indicate that $\tilde{K}(b_{\mathrm{T}})$ is basically negative, and that it becomes very negative at large b_{T}, so that the Fourier transform is well behaved.

Matching perturbative and non-perturbative parts

To match the perturbative and non-perturbative parts of $\tilde{D}$, we again use the quantity $\boldsymbol{b}_*$ defined in (13.59). Generalizing (13.60) we formulate an intrinsically non-perturbative part by the following decomposition:

$$\tilde{D}_{1,\,H_A/f}(z_A, b_{\mathrm{T}}; \zeta_A; \mu)$$

$$= \tilde{D}_{1,\,H_A/f}(z_A, b_*; \zeta_A; \mu) \left[\frac{\tilde{D}_{1,\,H_A/f}(z_A, b_{\mathrm{T}}; \zeta_A; \mu)}{\tilde{D}_{1,\,H_A/f}(z_A, b_*; \zeta_A; \mu)} \right]$$

$$= \tilde{D}_{1,\,H_A/f}(z_A, b_*; \zeta_A; \mu) \, \exp\left[-g_{H_A/f}(z_A, b_{\mathrm{T}}) - \ln\frac{\sqrt{\zeta_A}z_A}{m_A} g_K(b_{\mathrm{T}}) \right]. \qquad (13.68)$$

In the second line we simply separated out a factor of $\tilde{D}$ at b_*, which we will calculate perturbatively. We then evolved the fragmentation functions in the brackets to the reference values of ζ_A and μ. The effects of the anomalous dimension γ_D cancel between numerator and denominator, while from CS evolution there survived only the "non-perturbative" part of $\tilde{K}$, i.e., g_K, defined in (13.60). The remaining factor we chose to write as an exponential $e^{-g_{H_A/j}(z_A, b_{\mathrm{T}})}$, which we can label as the non-perturbative part of the intrinsic transverse momentum distribution (Fourier transformed).

The Fourier transform of (13.68) into momentum space should be well behaved under conditions when the factorization formula is used, i.e., when ζ_A is large enough, probably bigger than a few GeV^2. This implies that the function g_K should go to positive infinity as $b_{\mathrm{T}} \to \infty$. Typical fits assume that this behavior is proportional to one or two powers of b_{T}, i.e., that an exponential or Gaussian is appropriate. The constraints on the other function, $g_{H_A/j}$, are less severe. If its power law is the same as g_K, then there will be a problem when ζ_A is too low, since then the exponent would grow indefinitely at large b_{T}. This is not in principle a problem, since we should only use parton densities when a factorization formula is valid, i.e., only for ζ_A above some lower limit.

See Landry *et al.* (2003) and Konychev and Nadolsky (2006) for fits in the completely analogous case of TMD quark densities in a hadron.

To use the perturbative small-b_{T} result from (13.64), we now evolve the b_* factor (13.68) to a situation with no large kinematic ratios in the coefficient function $\tilde{C}$, whose logarithms

would prevent the effective use of perturbation theory. We therefore choose to replace μ_0 in (13.67) by

$$\mu_b = \frac{C_1}{b_*(b_\mathrm{T})}, \tag{13.69}$$

and we replace the reference value m_A^2/z_A^2 for ζ_A by μ_b^2. Then

$$\tilde{D}_{1,\,H_A/f}(z_A, b_\mathrm{T}; \zeta_A; \mu)$$

$$= \sum_j \int_{z_A}^1 \frac{\mathrm{d}\hat{z}}{\hat{z}^{3-2\epsilon}}\, d_{H_A/j}(\hat{z}; \mu_b)\; \tilde{C}_{j/f}\big(z_A/\hat{z}, b_*; \mu_b^2, \mu_b, g(\mu_b)\big)$$

$$\times \exp\!\left[-g_{H_A/f}(z_A, b_\mathrm{T}) - \ln\frac{\sqrt{\zeta_A}\,z_A}{m_A}\,g_K(b_\mathrm{T})\right]$$

$$\times \exp\!\left\{\ln\frac{\sqrt{\zeta_A}}{\mu_b}\,\tilde{K}(b_*; \mu_b) + \int_{\mu_b}^\mu \frac{\mathrm{d}\mu'}{\mu'}\left[\gamma_D(g(\mu'); 1) - \ln\frac{\sqrt{\zeta_A}}{\mu'}\gamma_K(g(\mu'))\right]\right\}. \tag{13.70}$$

This is probably the best formula for calculating and fitting TMD fragmentation functions; see (13.81) for its use in a factorization formula.[1] Besides the integrated fragmentation functions, which can be measured from simpler inclusive processes, there are further non-perturbative functions $g_{H_A/j}(z_A, b_\mathrm{T})$ and $g_K(b_\mathrm{T})$ that must be obtained by fits to data. The first of these functions requires essentially the same amount and kind of data to determine as we would need to determine TMD fragmentation functions if the simple parton model were valid, without any QCD modifications. The second function $g_K(b_\mathrm{T})$ depends only on a single variable, and can be obtained from the energy dependence of the process. Many predictions can be made with the aid of g_K, since it is independent of z_A, and also since exactly the same function appears in many other processes with TMD functions, both for fragmentation and for parton densities.

All remaining quantities are perturbative, and can therefore be predicted to useful accuracy from first principles by low-order Feynman-graph calculations. For this to work, the lower limit on μ_b, i.e., $C_1/b_{\max}$, should be at an energy scale where the use of perturbation theory is appropriate, say about 2 GeV. However, this is typically a fairly low scale, where the errors in truncated perturbation theory are substantially larger than in the calculation of the hard scattering at a scale of tens or hundreds of GeV. It is worth noting that because of the form of (13.70) these errors can dominantly be compensated by adjustments of the non-perturbative functions. That is, actual fits for the non-perturbative functions automatically compensate the largest higher-order terms in $\tilde{K}$ and $\tilde{C}$.

---

[1] In this application, ϵ is set to zero in the factor $1/\hat{z}^{3-2\epsilon}$. The ϵ dependence is retained in (13.70) so that the formula can also be related to regulated perturbative calculations.

13.12 Correction term for large $q_{h\mathrm{T}}$

The TMD factorization formalism described above applies when $q_{h\mathrm{T}}$ is treated as a small variable. Approximations were made that have errors of order a power of $q_{h\mathrm{T}}/Q$. When $q_{h\mathrm{T}}$ is of order Q, the conventional formalism, with its integrated fragmentation functions, is valid: Ch. 12. Notably, the large $q_{h\mathrm{T}}$ then arises from hard scattering with three or more final-state partons, whereas the TMD formalism associates $q_{h\mathrm{T}}$ with parton transverse momenta in the TMD fragmentation functions.

The TMD formalism loses accuracy at large $q_{h\mathrm{T}}$, with fractional errors we characterize as $(q_{h\mathrm{T}}/Q)^\alpha$. The other formalism loses accuracy at small $q_{h\mathrm{T}}$ with fractional errors $(m/q_{h\mathrm{T}})^\beta$, where m denotes a typical hadronic scale. In these estimates, α and β are positive powers for the first neglected terms in the region approximants, either 1 or 2 in reality, and we then can reduce these powers slightly so as to obtain errors valid in the presence of logarithmic corrections. We assume throughout that we do not let $q_{h\mathrm{T}}$ increase beyond order Q.

To work with the whole range of $q_{h\mathrm{T}}$ it is necessary to find a way of combining the two formalisms without loss of accuracy.

A simple-minded approach would be to use the TMD formalism for $q_{h\mathrm{T}}$ below some scale $Q_0 \ll Q$, and to use the conventional formalism above that scale. But this would substantially degrade the accuracy of the predictions. For example, suppose the error exponents are $\alpha = \beta = 1$. Then the worst fractional error in the use of the TMD formalism would be Q_0/Q, while that for the conventional formalism would be m/Q_0, both at $q_{h\mathrm{T}} = Q_0$. Globally optimal errors would be obtained with Q_0 proportional to the geometric mean of Q and m, for a fractional error of order $\sqrt{m/Q}$, i.e., with an error exponent 0.5 instead of unity.

Using the general principles of subtraction methods, Collins and Soper (1982a) devised a method that in principle gives m/Q errors for all $q_{h\mathrm{T}}$. Their idea was to treat the TMD term as a first approximation to the cross section (or structure function). It is obtained by applying a TMD approximator, T_{TMD}, to the structure function:

$$L = T_{\mathrm{TMD}} W^{\mu\nu}. \tag{13.71}$$

(Hidden inside the action of T_{TMD} are all the details of the extraction of the hard factor, the definitions of the TMD fragmentation function, etc.) This "low-transverse momentum term" L gives all but the Y term on the r.h.s. of (13.46).

The fractional error in the approximant is power-suppressed in $q_{h\mathrm{T}}/Q$:

$$|W - T_{\mathrm{TMD}} W| = O((q_{h\mathrm{T}}/Q)^\alpha |W|). \tag{13.72}$$

We define the correction term Y in (13.46) by applying an approximator for ordinary collinear factorization to the remainder:

$$Y \overset{\mathrm{def}}{=} T_{\mathrm{coll}}(W^{\mu\nu} - L) \tag{13.73}$$

The fractional errors in this approximation are suppressed by a factor $(m/q_{h\mathrm{T}})^\beta$. Although this degrades as $q_{h\mathrm{T}}$ gets small, it is applied to a quantity that itself is getting small. Therefore the sum of L and Y, i.e., the whole r.h.s. of (13.46), is a uniformly good approximation,

i.e., $W - L - Y$ is power-suppressed:

$$
\begin{aligned}
|W - L - Y| &= |(1 - T_{\text{coll}})(W - L)| \\
&= O\left((m/q_{h\,T})^{\beta}|W - L|\right) \\
&= O\left((m/q_{h\,T})^{\beta}(q_{h\,T}/Q)^{\alpha}|W|\right) \\
&= O\left((m/Q)^{\min(\alpha,\beta)}|W|\right).
\end{aligned}
\tag{13.74}
$$

The above error estimate applies when $q_{h\,T}$ is less than of order Q. However, although there is a kinematic limit at when $q_{h\,T}$ gets larger than Q, this kinematic limit is not respected by the low-$q_{h\,T}$ term. Its large-$q_{h\,T}$ behavior represents only a kind of extrapolation of the low-$q_{h\,T}$ behavior. Once one gets close to or beyond the kinematic limit, the error between W and L increases far beyond 100%. An appropriate solution is to redefine L with a cutoff to restrict the values of $q_{h\,T}$ to which it is applied. That is, L is replaced by

$$
L_F = F(q_{h\,T}/Q)\, T_{\text{TMD}} W.
\tag{13.75}
$$

Here the function $F(q_{h\,T}/Q)$ is chosen so that it is unity at $q_{h\,T} = 0$ and zero for large $q_{h\,T}$. A possible choice would be a theta function $F(q_{h\,T}/Q) = \theta(Q - q_{h\,T})$. A better choice would be a smooth function. Since the kinematic limit is dependent on the momentum fractions z_A and z_B, it would be appropriate to give corresponding dependence to the function F.

The cutoff function should be inserted in (13.46), multiplying its first term, and an appropriate redefinition of Y must be made:

$$
Y_F \overset{\text{def}}{=} T_{\text{coll}}(W - L_F).
\tag{13.76}
$$

If L and Y were computed exactly, the choice of cutoff function would be unimportant. But actual estimates of L and Y involve truncations of perturbation expansions, so the cutoff function F should be chosen to minimize errors, as well as these can be understood.

Other procedures are possible, for example as proposed by Arnold and Kauffman (1991). The overall aim is to minimize the likely errors of calculations.

13.13 Using TMD factorization

To use the factorization formalism we exploit the CS and RG evolution equations to change the values of μ and y_n in each factor separately, so that:

- perturbatively calculated quantities are applied in a region where their coefficients have no large logarithms;
- non-perturbative quantities are applied with fixed values of μ and Δy, so that the functions that need to be fitted to data have the minimum number of variables.

The resulting formula, (13.81) below, is suitable for data fitting and for using the results of perturbative calculations. However, this formula is quite complicated. So I show the factorization result in two other forms to exhibit the overall structure.

13.13.1 Three views of factorization

Main factorization formula

First is the main factorization formula, presented earlier (13.46), which follows most immediately from the derivation of factorization. It directly exhibits the low-$q_{h\,\mathrm{T}}$ part of the $W^{\mu\nu}$ in terms of TMD fragmentation functions. It is equivalent to a convolution of TMD fragmentation functions.

Factorization with fixed fragmentation functions

The fragmentation functions have dependence on auxiliary parameters as well as the momentum fractions and the transverse coordinates and momenta. We can exhibit factorization in terms of TMD densities at fixed reference values of the auxiliary parameters, by the use of (13.67), obtained from solving the CS and RG equations. This gives

$$
W^{\mu\nu} = \frac{8\pi^3 z_A z_B}{Q^2} \sum_f H_f^{\mu\nu}\big(Q; g(\mu_Q), \mu_Q\big) \int \frac{\mathrm{d}^2 \boldsymbol{b}_\mathrm{T}}{(2\pi)^2} e^{-i\boldsymbol{q}_{h\,\mathrm{T}}\cdot\boldsymbol{b}_\mathrm{T}} e^{-S(b_\mathrm{T};Q;\mu_Q,\mu_0)}
$$

$$
\times \tilde{D}_{1,\,H_A/f}\left(z_A, b_\mathrm{T}; \frac{m_A^2}{z_A^2}; \mu_0\right) \tilde{D}_{1,\,H_B/\bar{f}}\left(z_B, b_\mathrm{T}; \frac{m_B^2}{z_B^2}; \mu_0\right)
$$

$$
+ \text{polarized terms} + \text{large-}q_{h\,\mathrm{T}} \text{ correction, } Y. \tag{13.77}
$$

We now have fixed fragmentation functions combined with an allowance for recoil against energy-dependent gluon emission, in the factor

$$
e^{-S(b_\mathrm{T};Q;\mu_Q,\mu_0)} \overset{\text{def}}{=} \exp\left\{\ln\frac{Q^2 z_A z_B}{m_A m_B} \tilde{K}(b_\mathrm{T};\mu_0)\right\}
$$

$$
\times \exp\left\{\int_{\mu_0}^{\mu_Q} \frac{\mathrm{d}\mu'}{\mu'}\left[2\gamma_D(g(\mu');1) - \ln\frac{Q^2}{(\mu')^2}\gamma_K(g(\mu'))\right]\right\}, \tag{13.78}
$$

where the first factor gives an energy-dependent shape to the TMD distribution, but the second factor only affects the normalization. Observe that all dependence on y_n has disappeared.

In (13.77) the renormalization scale in the hard factor $H_f^{\mu\nu}$ is chosen to be proportional to Q,

$$
\mu_Q = C_2 Q. \tag{13.79}
$$

This is used to minimize logarithms in perturbative calculations of $H_f^{\mu\nu}$, which is obtained as a (Dirac and color) trace over on-shell hard-scattering amplitudes:

$$
H_f^{\mu\nu}(Q; g(\mu), \mu) = \operatorname{Tr} k_A^+ \gamma^- H_f^\nu(Q) k_B^- \gamma^+ \overline{H}_f^\mu(Q). \tag{13.80}
$$

Factorization with maximum perturbative content

Finally, we apply the small-b_T perturbative expansion of the TMD fragmentation functions in the form of (13.70), where it is combined with functions to parameterize the non-perturbative large b_T dependence. This gives

$$W^{\mu\nu} = \frac{8\pi^3 z_A z_B}{Q^2} \sum_{f, j_A, j_B} H^{\mu\nu}_f\big(Q; g(\mu_Q), \mu_Q\big) \int \frac{\mathrm{d}^2 \boldsymbol{b}_T}{(2\pi)^2} e^{-i\boldsymbol{q}_{h\,T}\cdot\boldsymbol{b}_T}$$

$$\times \int_{z_A}^1 \frac{\mathrm{d}\hat{z}_A}{\hat{z}_A^3} d_{H_A/j_A}(\hat{z}_A; \mu_b) \, \tilde{C}_{j_A/f}\left(\frac{z_A}{\hat{z}_A}, b_*; \mu_b^2, \mu_b, g(\mu_b)\right)$$

$$\times \int_{z_B}^1 \frac{\mathrm{d}\hat{z}_B}{\hat{z}_B^3} d_{H_B/j_B}(\hat{z}_B; \mu_b) \, \tilde{C}_{j_B/\bar{f}}\left(\frac{z_B}{\hat{z}_B}, b_*; \mu_b^2, \mu_b, g(\mu_b)\right)$$

$$\times \exp\big[-g_{H_A/f}(z_A, b_T) - g_{H_B/\bar{f}}(z_B, b_T)\big]$$

$$\times \exp\left[-\ln\frac{Q^2 z_A z_B}{m_A m_B} g_K(b_T) + \ln\frac{Q^2}{\mu_b^2}\tilde{K}(b_*; \mu_b)\right]$$

$$\times \exp\left\{\int_{\mu_b}^{\mu_Q} \frac{\mathrm{d}\mu'}{\mu'}\left[2\gamma_D(g(\mu'); 1) - \ln\frac{Q^2}{(\mu')^2}\gamma_K(g(\mu'))\right]\right\}$$

$$+ \text{polarized terms} + \text{large-}q_{h\,T} \text{ correction}, Y. \tag{13.81}$$

The second and third lines are the part contributed by the integrated fragmentation functions. At lowest order

$$\text{Lines 2 and 3 of (13.81)} \overset{\text{LO}}{=} \frac{d_{H_A/f}(z_A; \mu_b) \, d_{H_B/\bar{f}}(z_B; \mu_b)}{z_A^2 z_B^2} + O(\alpha_s(\mu_b)). \tag{13.82}$$

The fourth line of (13.81) gives the non-perturbative contribution to the non-evolving part of the transverse distributions. Finally, the last two lines give the effect of gluon radiation, perturbative and non-perturbative.

The overall non-perturbative factor has the form

$$\exp\left[-g_{H_A/f}(z_A, b_T) - g_{H_A/\bar{f}}(z_B, b_T) - \ln\frac{Q^2 z_A z_B}{m_A m_B} g_K(b_T)\right]. \tag{13.83}$$

This represents the TMD part that must (currently) be obtained by fitting to data. It concerns the region of large b_T. To avoid interfering with the results of valid perturbative calculations, the functions in the exponent should decrease like a power of b_T at *small b_T*. The choice giving the logarithm in (13.83) (and the corresponding logarithm in (13.81)) was explained below (13.67).

13.13.2 Arbitrariness in renormalization scales and $b_{\max}$

In the perturbative parts of (13.81), there are choices of the scales μ_b and μ_Q, with an arbitrariness parameterized by the coefficients C_1 and C_2. As is usual with a choice

of renormalization/factorization scale, if all the factors were calculated exactly, then the result for $W^{\mu\nu}$ would be independent of C_1 and C_2. This follows simply from the CS and RG evolution equations treated exactly. But the perturbative calculations of the various quantities needed, H, $\tilde{C}$, $\tilde{K}$, γ_D and γ_K, are always truncated finite-order calculations. So there is residual dependence on C_1 and C_2 due to truncation errors. This dependence is small if the truncation errors are small. The coefficients should be chosen to minimize truncation errors, which can only be done approximately in the absence of exact calculations. My own approach to estimating appropriate values of renormalization scales is summarized in Sec. 3.4.

The remaining arbitrary parameter is $b_{\max}$, which roughly characterizes the boundary between the non-perturbative and perturbative domains for b_T dependence. The dependence on $b_{\max}$ arises from the dependence of the definition of $\boldsymbol{b}_*(\boldsymbol{b}_T)$ on $b_{\max}$.

In (13.81), there is explicit dependence on b_* only in the $\tilde{C}$ factors and in $\tilde{K}$. There is also dependence via the dependence of many quantities on μ_b; see (13.69). But we have already seen that the μ_b dependence cancels up to perturbative truncation errors. The explicit dependence on b_* is in places where it can be exactly compensated by a change in the functional form of the non-perturbative functions $g_{H_A/f}$, $g_{H_B/\bar{f}}$, and g_K.

Therefore a change of $b_{\max}$ in no way affects the fundamental validity of the formalism, but only the extent to which perturbation theory is used to predict the b_T dependence. However, fits of the non-perturbative functions are normally made by postulating particular functional forms, e.g., (14.38) below, with a small number of parameters. In principle, if such a parameterization is accurate at one value of $b_{\max}$, it will become invalid when $b_{\max}$ is changed. How much of a practical issue this is, needs an examination of actual fits. See Sec. 14.5.3 for further comments.

13.13.3 Fitting data, etc.

It would be interesting to see how (13.81) compares to actual experimental data. However, the most developed phenomenology is for the Drell-Yan process, which we will treat later. See Sec. 14.5 for the factorization formalism, which has the same general structure as for the two-hadron-inclusive cross section in e^+e^- annihilation. A review of the phenomenology for the Drell-Yan process is given in Sec. 14.5.3.

13.13.4 Leading-logarithm approximation

One method of analyzing a process with a large scale is to determine in each order of perturbation theory the term with the highest power of a logarithm. These leading logarithms can often be derived analytically. The leading-logarithm approximation (LLA) is the sum of these terms, and it is often treated as a useful approximation to the exact result, because it sums the biggest terms in the perturbation expansion. In a strict LLA, the coupling is treated as fixed. In the b_T-space integrand, (13.81), the leading logarithms for large Qb_T are the two per loop associated with the leading order γ_K. Relative to a pure LO result, we

have a factor

$$W_{\text{LLA}}(b; Q) = \exp\left(-\frac{g^2(\mu)}{\pi^2}C_F\int_{1/b}^{Q}\frac{d\mu'}{\mu'}\ln\frac{Q}{\mu'}\right)d_{H_A/f}(z_A; \mu)\,d_{H_B/\bar{f}}(z_B; \mu).$$

$$= \exp\left(-\frac{g^2(\mu)}{2\pi^2}C_F\ln^2(Qb)\right)d_{H_A/f}(z_A; \mu)\,d_{H_B/\bar{f}}(z_B; \mu). \qquad (13.84)$$

This exhibits all the main qualitative features just described. The value of μ and hence the value of the coupling are not determined within the LLA. The choice of an appropriate value needs some intuition. One natural choice is that $\mu = 1/b_{\text{peak}}$, where b_{peak} is the maximum of $bW(b, Q)$, so μ is the solution of $\ln(Q/\mu) = 2\pi^2/(g^2(\mu)C_F)$.

The LLA can also be obtained in transverse momentum space, for example by Fourier transformation of each term in the LLA in b_{T} space. This gives

$$\frac{d\sigma}{d^2\boldsymbol{q}_{h\,\text{T}}} \propto \frac{g^2C_F\ln\frac{Q}{q_{h\text{T}}}\exp\left(-\frac{g^2(\mu)}{2\pi^2}C_F\ln^2(Q/q_{h\text{T}})\right)}{q_{h\text{T}}^2}d_{H_A/f}(z_A; \mu)\,d_{H_B/\bar{f}}(z_B; \mu)$$

$$= \frac{g^2C_F\ln\frac{Q}{q_{h\text{T}}}}{q_{h\text{T}}^2}\left(\frac{q_{h\text{T}}}{Q}\right)^{\frac{g^2(\mu)}{2\pi^2}C_F\ln(Q/q_{h\text{T}})}d_{H_A/f}(z_A; \mu)\,d_{H_B/\bar{f}}(z_B; \mu). \qquad (13.85)$$

This last formula serves as an excellent warning about the inadequacies of the leading-logarithm method, despite its widespread use and tacit acceptance. Without the logarithms, the cross section diverges like $1/q_{h\text{T}}^2$ as $q_{h\text{T}} \to 0$. But with the resummed logarithms, the cross section decreases to zero faster than any power of $q_{h\text{T}}$, as exhibited on the second line. This contradicts the correct result, which is that the cross section is finite and non-zero at $q_{h\text{T}} = 0$. Even the LLA in b_{T} space implies this result.

The LLA can indeed provide some semi-quantitative information when the logarithms are not too large, by focusing attention on the largest terms in the perturbation expansion. One of the dangers of taking the LLA too literally is indicated by the Fourier transformation. Even if the LLA in b_{T} space were appropriate, the LLA in $q_{h\text{T}}$ space need not be.

In general, there is no justification for using the LLA beyond some limited domain where $\frac{g^2(\mu)}{2\pi^2}C_F\ln^2(Q/q_{h\text{T}}) \lesssim 1$. In contrast the derivation of the TMD factorization theorem is intended to be valid all the way down to $\boldsymbol{q}_{h\,\text{T}} = 0$.

13.13.5 Resummation methodology

The LLA presents some quantity like $W(b)$ or a cross section as a sum over all orders of perturbation theory, with each order being calculated as some analytically tractable approximation to full perturbation theory. This is called a "resummation" of perturbation theory.

In the literature can be found many generalizations of such resummations, for example to allow for a running coupling. Indeed TMD factorization formulae like (13.81) are often claimed to be resummation formulae: the starting point in this viewpoint is the *normal, collinear* factorization formula valid at large transverse momentum, i.e., at $q_{h\,\text{T}} \sim Q$. In

the hard-scattering coefficient H, higher-order terms contain logarithms of $Q/q_{h\,T}$, as in (13.85). Of course, when $q_{h\,T}$ is too small, the logarithms prevent the reliable use of fixed-order perturbation theory, and resummation tries to overcome this problem.

If the logarithms are large but not too large, the use of resummation is reasonable. However, the justification for using *collinear* factorization as a starting point breaks down if one takes $q_{h\,T}$ too small. Now the first part of the derivation was a region analysis of amplitudes, and this remains valid for arbitrarily small $q_{h\,T}$, provided that Q stays large. However, there is a failure of the approximations that led to the hard scattering and to the definitions of integrated parton densities and fragmentation functions. Parts of the approximations neglect partonic transverse momentum and virtuality, not just relative to Q, but also relative to $q_{h\,T}$. The partonic transverse momenta at issue are those intrinsically associated with the hadronic mass scale, so the actual (fractional) errors in collinear factorization are a power of $M/q_{h\,T}$.

Generally collinear factorization also applies to the *integral* of the cross section over $q_{h\,T}$, since the relevant errors in the approximations merely redistribute the cross section as a function $q_{h\,T}$.

In deriving TMD factorization, we have carefully preserved transverse momentum kinematics, and so the errors become a power of M/Q instead of $M/q_{h\,T}$. TMD factorization then applies all the way down to zero $q_{h\,T}$.

A less abstract way to see the problems with applying collinear factorization (resummed or not) at small $q_{h\,T}$ is from the existence of an unphysical $1/q_{h\,T}^2$ singularity at $q_{h\,T} = 0$ in each order of the perturbative expansion of the hard-scattering factor in collinear factorization. Each of the summed terms in LLA is representative of the singularity. But the singularity (with its associated logarithms) arises from emission of collinear and soft emission gluons from parent partons that are *exactly* massless and on-shell. In physical reality such partons do not exist.

There is a further problem with an LLA such as (13.84) or (13.85), that the terms alternate in sign and exponentiate to a result much smaller than the first term when $b_T \gg 1/Q$. or $q_{h\,T} \ll Q$. Without further knowledge, one could not exclude that some non-leading logarithm might be outside the exponential form, e.g., a single term $\alpha_s^{10}/q_{h\,T}^2$ *added* to an exponential series such as in (13.85). This term is of such high order that in practice it would probably not be calculable. Without an accompanying exponential of even higher-order terms, this high order would completely dominate the LLA sum.

Essentially full TMD factorization does ensure that higher-order terms can be organized so that there is an exponential factor. But the exponentials are the rather different ones in (13.81), and give rather different behavior than the LLA at zero $q_{h\,T}$.

13.14 NLO calculation of TMD fragmentation function at small b_T and at large k_T

To calculate the coefficient functions for the small-b_T fragmentation functions, we make the usual observation that the coefficient functions are independent of the type of the detected hadron. Thus we can (a) replace the hadron by a parton in IR-regulated massless QCD,
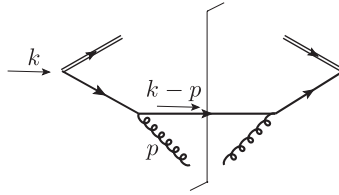
Fig. 13.7. One-loop fragmentation of quark to a gluon of *physical* polarization. The diagram applies equally to TMD and integrated fragmentation functions.

(b) compute both the TMD and the integrated fragmentation functions in strict fixed-order perturbation, and then (c) deduce the coefficient functions at that order from the perturbative expansion of (13.64).

For each of the functions, let the expansion in powers of the *renormalized* coupling be notated like

$$\tilde{C}_{j/f} = \sum_{n=0}^{\infty} \left(\frac{g^2}{16\pi^2} \right)^n \tilde{C}_{j/f}^{[n]}. \tag{13.86}$$

We write factorization (13.64) in a convolution notation as $\tilde{D} = d \otimes C$.

Then the first-order terms give

$$d^{[0]} \otimes \tilde{C}^{[1]} = \tilde{D}^{[1]} - d^{[1]} \otimes \tilde{C}^{[0]}. \tag{13.87}$$

The lowest-order coefficient $\tilde{C}^{[0]}$ is given in (13.65), and the lowest-order integrated fragmentation function is

$$d_{j/j'}^{[0]}(z) = \delta_{jj'}\delta(z - 1), \tag{13.88}$$

so that

$$\tilde{C}_{j/f}^{[1]}(z, \boldsymbol{b}_{\mathrm{T}}) = \tilde{D}_{j/f}^{[1]}(z, \boldsymbol{b}_{\mathrm{T}}) - \frac{d_{j/f}^{[1]}(z)}{z^{2-2\epsilon}}, \tag{13.89}$$

where the denominator in the last term arises from the $\hat{z}^{3-2\epsilon}$ denominator of the measure in the convolution, (13.64), which in turn arises from the different powers of z in the definitions of TMD and integrated fragmentation functions, e.g., (12.39) and (12.40).

In the above formulae, j and f represent any parton type. We will compute the one-loop corrections for the cases that f is any flavor of quark, since these are the relevant ones in TMD factorization of the two-particle-inclusive cross section.

13.14.1 Gluon from quark at $O(g^2)$

The sole graph we need to calculate the fragmentation of a quark to a gluon at $O(g^2)$ is shown in Fig. 13.7. The hadron-frame momentum of the gluon is $p_h = (p_h^+, 0, \boldsymbol{0}_{\mathrm{T}}) = (zk_h^+, 0, \boldsymbol{0}_{\mathrm{T}})$, and we restrict to a sum over physical polarizations, chosen to be in the transverse plane. Then we have no graphs in which the gluon connects to a Wilson line.

For the dimensionally regulated TMD fragmentation function, we have

$$
\frac{g^2}{16\pi^2} \tilde{D}^{[1]}_{g/q}(z, \boldsymbol{b}_{\mathrm{T}}) = \frac{g^2 \mu^{2\epsilon} C_F}{(2\pi)^{4-2\epsilon} z} \int \mathrm{d}k^- \, \mathrm{d}^{2-2\epsilon} \boldsymbol{k}_{\mathrm{T}} \, e^{i\boldsymbol{k}_{\mathrm{T}} \cdot \boldsymbol{b}_{\mathrm{T}}} 2\pi \delta\big((k-p^2)\big)
$$

$$
\times \frac{\frac{1}{4} \mathrm{Tr} \sum_j \gamma^+ \slashed{k} \gamma^j (\slashed{k} - \slashed{p}) \gamma^j \slashed{k}}{(k^2)^2}
$$

$$
= \frac{g^2 (4\pi^2 \mu^2)^\epsilon C_F}{8\pi^3} \int \frac{\mathrm{d}^{2-2\epsilon} \boldsymbol{k}_{\mathrm{T}} \, e^{i\boldsymbol{k}_{\mathrm{T}} \cdot \boldsymbol{b}_{\mathrm{T}}}}{k_{\mathrm{T}}^2} \left[\frac{1 + (1-z)^2 - \epsilon z^2}{z^3} \right]. \quad (13.90)
$$

In the first line, the sum over j is over all transverse indices. There is a (collinear) divergence at $k_{\mathrm{T}} = 0$, which is regulated if $\epsilon < 0$.

For the integrated function, the same formula applies, except that (a) the factor $1/z$ in the definition (12.39) is changed to $z^{1-2\epsilon}$, as in (12.40), (b) $\boldsymbol{b}_{\mathrm{T}}$ is set to zero, and (c) an $\overline{\mathrm{MS}}$ renormalization counterterm is used to cancel the resulting UV divergence:

$$
\frac{g^2}{16\pi^2} d^{[1]}_{g/q}(z) = \frac{g^2 (4\pi^2 \mu^2)^\epsilon C_F}{8\pi^3} \int \frac{\mathrm{d}^{2-2\epsilon} \boldsymbol{k}_{\mathrm{T}}}{k_{\mathrm{T}}^2} \left[\frac{1 + (1-z)^2 - \epsilon z^2}{z^{1+2\epsilon}} \right]
$$

$$
- \frac{g^2 C_F S_\epsilon}{8\pi^2 \epsilon} \left[\frac{1 + (1-z)^2}{z} \right]. \quad (13.91)
$$

Using (13.89), we find the one-loop coefficient function

$$
\frac{g^2}{16\pi^2} \tilde{C}^{[1]}_{g/q}(z, \boldsymbol{b}_{\mathrm{T}})
$$

$$
= \frac{g^2 (4\pi^2 \mu^2)^\epsilon C_F}{8\pi^3} \int \frac{\mathrm{d}^{2-2\epsilon} \boldsymbol{k}_{\mathrm{T}} (e^{i\boldsymbol{k}_{\mathrm{T}} \cdot \boldsymbol{b}_{\mathrm{T}}} - 1)}{k_{\mathrm{T}}^2} \left\{ \frac{1 + (1-z)^2 - \epsilon z^2}{z^3} \right\}
$$

$$
+ \frac{g^2 C_F S_\epsilon}{8\pi^2 \epsilon} \left[\frac{1 + (1-z)^2}{z^{3-2\epsilon}} \right]
$$

$$
= \frac{g^2 C_F}{8\pi^2} \left(\pi b_{\mathrm{T}}^2 \mu^2 \right)^\epsilon \Gamma(-\epsilon) \left\{ \frac{1 + (1-z)^2 - \epsilon z^2}{z^3} \right\} + \frac{g^2 C_F S_\epsilon}{8\pi^2 \epsilon} \left[\frac{1 + (1-z)^2}{z^{3-2\epsilon}} \right]
$$

$$
\stackrel{\epsilon=0}{=} \frac{g^2 C_F}{8\pi^2 z^3} \left\{ 2 \left[1 + (1-z)^2 \right] \left[\ln \frac{2z}{\mu b_{\mathrm{T}}} - \gamma_{\mathrm{E}} \right] + z^2 \right\}. \quad (13.92)
$$

In the first line, the collinear divergence at $k_{\mathrm{T}} = 0$ is exactly canceled, and in the second line the UV divergence $k_{\mathrm{T}} = \infty$ is renormalized. The integral was performed using (A.45).

Notice that if we applied $\int \mathrm{d}^{2-2\epsilon} \boldsymbol{k}_{\mathrm{T}} / k_{\mathrm{T}}^2 = 0$ in the first line, then we would be left with the IR-divergent integral $\int \mathrm{d}^{2-2\epsilon} \boldsymbol{k}_{\mathrm{T}} \, e^{i\boldsymbol{k}_{\mathrm{T}} \cdot \boldsymbol{b}_{\mathrm{T}}} / k_{\mathrm{T}}^2$. The $\overline{\mathrm{MS}}$ counterterm would appear to be canceling the IR divergence (strictly a collinear divergence). Although this method of IR cancellation corresponds to much actual calculational practice, it does not reflect the correct conceptual treatment.

After Fourier transformation of (13.92) back to momentum space, the behavior of the TMD at large transverse momentum is determined by the singularity in the Fourier conjugate variable, i.e., by the logarithm of b_{T}. Much more simply, one just inverts the
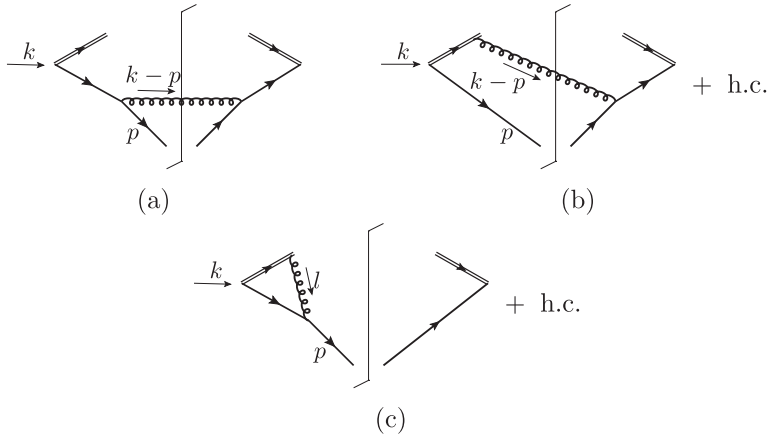
Fig. 13.8. One-loop fragmentation of quark from quark. For the TMD functions, there are also the Wilson-line terms shown in Fig. 13.9.

Fourier transform in the first line of (13.92), to obtain

$$\frac{g^2}{16\pi^2} C_{g/q}^{[1]}(z, \boldsymbol{k}_{\mathrm{T}}) = \frac{g^2 C_F}{8\pi^3} \frac{1 + (1-z)^2}{k_{\mathrm{T}}^2 z^3} \qquad \text{(at large } k_{\mathrm{T}}\text{).} \qquad (13.93)$$

13.14.2 Quark from quark at $O(g^2)$

For the quark-to-quark fragmentation function, we use the graphs shown in Fig. 13.8. These need some explanation. The Wilson line is in the light-like direction $w_B = (0, 1, \boldsymbol{0}_{\mathrm{T}})$. It is now the outgoing quark that is detected and that has zero transverse momentum. Since the gluon has non-zero transverse momentum, its physical polarizations are no longer exactly in the transverse plane, and its coupling to the Wilson line is non-zero. It is convenient to calculate using a sum over all gluon polarizations, physical and unphysical, with the polarization sum $-g_{\kappa\lambda}$. The unphysical part cancels between graphs, by a standard textbook argument. Although quark self-energy graphs contribute to the actual one-loop fragmentation functions, they cancel in the difference used to compute the coefficient function in (13.89).

For the TMD quark fragmentation function, the graphs shown are for the $\tilde{D}^{\mathrm{unsub}}$ factor in the definition (13.42). We must add the one-loop contribution of the soft factor part of the definition, i.e., the graphs in Fig. 13.9, and these last graphs are to be multiplied by the lowest-order fragmentation function of a quark to a quark, i.e., $\delta(z - 1)$. They cancel a rapidity divergence that will manifest itself in a singularity at $z = 1$ in Fig. 13.8. We also add renormalization counterterms to cancel UV divergences in all the virtual graphs, i.e., for Figs. 13.8(c) and 13.9(b).

For the integrated fragmentation function, we need only the graphs of Fig. 13.8, which now all have an unrestricted integral over transverse momentum. With this unrestricted integral, the rapidity divergences cancel between real and virtual gluon emission. We also
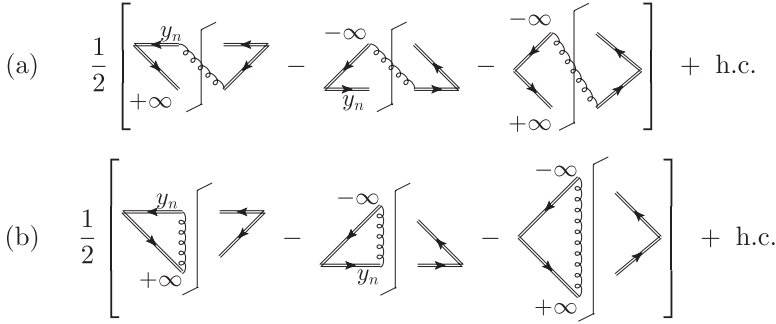
Fig. 13.9. One-loop graphs for soft-factor contributions to quark-to-quark fragmentation. The labels next to the Wilson lines indicate their rapidities. The graphs are to be multiplied by the zeroth-order fragmentation function $\delta(z-1)$.

need counterterms to cancel the UV divergences from the integral to infinite transverse momentum.

Since the graphs of Fig. 13.8 are doing double duty, for the two kinds of fragmentation function, I first summarize the overall calculational structure to obtain $\tilde{C}_{q/q}^{[1]}$:

Fig. 13.8 for TMD f.f. $+$ (Fig. $13.9 \times \delta(z-1)$) $+ \overline{\text{MS}}$ c.t.

$$- z^{-2+2\epsilon}\big[\text{Fig. 13.8 for integrated f.f.} + \overline{\text{MS}} \text{ c.t.}\big]. \quad (13.94)$$

The contribution of Fig. 13.8(a) to the dimensionally regulated TMD fragmentation function is straightforwardly

$$\frac{g^2(4\pi^2\mu^2)^\epsilon C_F}{8\pi^3} \frac{(1-z)(1-\epsilon)}{z^2} \int \mathrm{d}^{2-2\epsilon}\boldsymbol{k}_\mathrm{T} \frac{e^{i\boldsymbol{k}_\mathrm{T}\cdot\boldsymbol{b}_\mathrm{T}}}{k_\mathrm{T}^2}. \quad (13.95)$$

Graph (b) (including its hermitian conjugate) is

$$\frac{g^2(4\pi^2\mu^2)^\epsilon C_F}{8\pi^3} \frac{2}{z(1-z)} \int \mathrm{d}^{2-2\epsilon}\boldsymbol{k}_\mathrm{T} \frac{e^{i\boldsymbol{k}_\mathrm{T}\cdot\boldsymbol{b}_\mathrm{T}}}{k_\mathrm{T}^2}. \quad (13.96)$$

This has a singularity at $z = 1$. In the integral in the factorization formula, the singularity is at $z_A/\hat{z} = 1$, an endpoint of the integration over $\hat{z}$. The singularity is from a rapidity divergence associated with the light-like Wilson line. The rapidity divergence is canceled by the contribution from Fig. 13.9(a). This contribution is calculated almost identically to the corresponding term for the Sudakov form factor, and corresponds to the last three terms in the braces in (10.136). The differences are that (a) the gluon propagator is cut, (b) we add a hermitian conjugate term, (c) there is a group theory factor, and (d) we set masses to zero, obtaining:

$$-\frac{g^2(4\pi^2\mu^2)^\epsilon C_F}{8\pi^3} 2\delta(z-1) \int \mathrm{d}^{2-2\epsilon}\boldsymbol{k}_\mathrm{T}\, e^{i\boldsymbol{k}_\mathrm{T}\cdot\boldsymbol{b}_\mathrm{T}} \int_0^\infty \frac{\mathrm{d}l^+}{l^+} \Re \frac{1}{k_\mathrm{T}^2 - 2(l^+)^2 e^{-2y_n} - i0}. \quad (13.97)$$

Here l^+ is the plus momentum of the gluon, and there is a rapidity divergence at $l^+ = 0$. Because the soft factor (13.23) is defined with an integral over all k_S^+ and k_S^-, there is no dependence of (13.97) on external plus momenta. Thus the integral over l^+ ranges to infinity rather than a finite value. A real part $\Re$ is applied, because of the addition of the hermitian conjugate graphs.

To cancel the rapidity divergences, we combine (13.96) and (13.97) using the same distributional technique as we used in Sec. 9.4.4 in the renormalization of the quark parton density. After that the l^+ integral in (13.97) is made convergent and can be performed analytically. Combining all the graphs so far gives

$$
\frac{g^2 (4\pi^2 \mu^2)^\epsilon C_F}{8\pi^3} \int d^{2-2\epsilon} \boldsymbol{k}_T \, \frac{e^{i\boldsymbol{k}_T \cdot \boldsymbol{b}_T}}{k_T^2}
$$
$$
\times \left[\left(\frac{2}{1-z} \right)_+ + \frac{2}{z} + \frac{(1-z)(1-\epsilon)}{z^2} + \delta(z-1) \ln \frac{2(k^+)^2 e^{-2y_n}}{k_T^2} \right]. \tag{13.98}
$$

The IR/collinear divergence at $k_T = 0$ will cancel against the contribution of the integrated fragmentation function. But we will not display this explicitly. Instead we will proceed calculationally. All the remaining graphs, i.e., not only the virtual graphs for TMD fragmentation function, i.e., Figs. 13.8(c) and 13.9(b), but also all the graphs for the integrated fragmentation function, give zero, because they have scale-free transverse-momentum integrals.

So it remains to add the UV counterterms, whose total contribution is

$$
\frac{g^2 C_F}{8\pi^2} \left\{ \delta(z-1) \left[-\frac{S_\epsilon}{\epsilon^2} + \frac{S_\epsilon}{\epsilon} \left(\ln \frac{2(k^+)^2 e^{-2y_n}}{\mu^2} - 2 \right) \right] \right.
$$
$$
\left. + z^{-2+2\epsilon} \frac{S_\epsilon}{\epsilon} \left[\left(\frac{2}{1-z} \right)_+ - 1 - z + 2\delta(z-1) \right] \right\}. \tag{13.99}
$$

The first line has the counterterms for the TMD fragmentation function's virtual graphs; their calculation is the same as for the Sudakov form factor (10.139), except for a group-theory factor C_F and except for multiplication by 2 and removal of the imaginary part. The second line has the counterterms for the integrated fragmentation function; these are the same as the DGLAP kernel, but without the contribution associated with the quark self-energy graph.

Then we perform the $\boldsymbol{k}_T$ integrals analytically and add everything together at $\epsilon = 0$, to obtain

$$
\frac{g^2}{16\pi^2} \tilde{C}_{j'/j}^{[1]}(z, \boldsymbol{b}_T) \stackrel{\epsilon=0}{=} \frac{g^2 C_F \delta_{j'j}}{8\pi^2} \left(2 \left[\left(\frac{2}{1-z} \right)_+ + \frac{1}{z^2} + \frac{1}{z} \right] \left[\ln \frac{2z}{\mu b_T} - \gamma_E \right] \right.
$$
$$
+ \frac{1}{z^2} - \frac{1}{z} + \delta(z-1) \left\{ -\frac{1}{2} \left[\ln(\mu^2 b_T^2) - 2(\ln 2 - \gamma_E) \right]^2 \right.
$$
$$
\left. \left. - \left[\ln(\mu^2 b_T^2) - 2(\ln 2 - \gamma_E) \right] \ln \frac{2(k^+)^2 e^{-2y_n}}{\mu^2} \right\} \right). \tag{13.100}
$$

For generality, we have allowed arbitrary quark flavors j and j', with, of course, a Kronecker delta between them. Notice that there are *two* logarithms of b_T in this one-loop calculation, associated with the presence of a Sudakov form factor.

Correspondingly on Fourier transformation back to momentum space, there is a logarithm of k_T in the large-k_T behavior:

$$\frac{g^2}{16\pi^2} C^{[1]}_{j'/j}(z, \boldsymbol{k}_T) \stackrel{\epsilon=0}{=} \frac{g^2 C_F \delta_{j'j}}{8\pi^3} \frac{1}{k_T^2}$$

$$\times \left[\left(\frac{2}{1-z} \right)_+ + \frac{1}{z} + \frac{1}{z^2} + \delta(z-1) \ln \frac{2(k^+)^2 e^{-2y_n}}{k_T^2} \right], \quad (13.101)$$

obtained most easily from (13.98).

13.14.3 Failure of positivity

As initially defined, a TMD fragmentation function had the meaning of a number density of a hadron in a parton. This would imply that the coefficient function $C(z, \boldsymbol{k}_T)$ is also positive. However, the $\ln k_T$ in (13.101) ensures that the coefficient becomes negative (at $z = 1$) when k_T is larger than $\sqrt{2}k^+ e^{-y_n}$, which we normally choose to be approximately the overall CM energy Q. There is a subsidiary positivity problem that the distribution $1/(1-z)_+$ is not positive, because it is defined with a subtraction. When (13.101) is convoluted with an integrated fragmentation function, to get the TMD fragmentation function, there is a combination of positive and negative terms. But at sufficiently large k_T the negative delta-function term dominates, and positivity is violated.

Note that the quark-to-gluon coefficient (13.93) has no such problem, because it has neither a logarithm nor a plus distribution.

The resolution of the problem starts by the observation that we were forced to modify the definition of the TMD fragmentation function from its naive one. We made subtractions, notably to remove the contribution of rapidity divergences. Since we used subtractions rather than a cutoff, we can get a negative value, just as in our implementation in Sec. 3.4 of renormalization by subtraction of an asymptote.

The real positivity requirement is on cross sections. The TMD functions occur by themselves only in a factorization theorem for $q_{hT} \ll Q$, where small values of parton transverse momenta dominate. In that region, the logarithm at issue is indeed positive.

For large q_{hT} the TMD factorization formula represents only part of an estimate of the cross section. To compensate the error, we devised a correction term Y in Sec. 13.12. It corrects the cross section to the one obtained from standard collinear factorization, and is available to compensate the negativity in one individual term.

Obtaining a positive physical cross section from a combination of terms of opposite sign can be dangerous numerically, since the negative term can be larger than the final answer. It would not be a real issue if we could calculate exactly all the coefficients involved, to all orders of perturbation theory. But there can practical difficulties with low-order estimates.
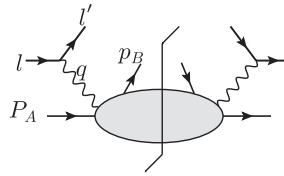
Fig. 13.10. SIDIS cross section.

This suggests that modifications of the basic formalism would be useful; see Sec. 13.12 and Arnold and Kauffman (1991). Any modification should agree with the TMD form of factorization at small $q_{h\,T}$ and should agree with normal collinear factorization at large $q_{h\,T}$. But creativity in combining and/or matching the two kinds of contribution without double counting is appropriate.

13.14.4 Other cases

By charge-conjugation invariance, the above coefficients are unchanged if the quark (of any flavor) is changed to an antiquark.

   At one loop, there is zero coefficient to get a quark from an antiquark, or vice versa. This process needs a minimum of two loops.

   The coefficients for quark from gluon and gluon from gluon are left as an exercise. These cases are *currently* of lesser experimental importance, since the main currently studied reactions sensitive to TMD fragmentation are those where the hard scattering involves quarks (and antiquarks). These reactions are e^+e^- annihilation, SIDIS and Drell-Yan.

13.15 SIDIS and TMD parton densities

So far, we treated TMD factorization for reactions in e^+e^- annihilation, where TMD fragmentation functions were used. We now extend these ideas to a process that needs parton densities, specifically semi-inclusive DIS (SIDIS). Another process that uses TMD parton densities is the Drell-Yan process to be treated in Ch. 14 along with the complications in obtaining factorization in hadron-hadron collisions.

   The results for SIDIS are a straightforward generalization of those for e^+e^- annihilation, so it is mainly necessary to explain the changes.

13.15.1 Kinematics

Semi-inclusive deeply inelastic scattering (SIDIS) is DIS with inclusive measurement of one hadron as well as a lepton in the final state: $e(l) + H_A(P_A) \rightarrow e(l') + H_B(p_B) + X$, Fig. 13.10. We choose the outgoing lepton to be in the DIS region, so that the reaction has large Q, and we also choose the hadron H_B to be in a region where it can be a fragmentation product of one of the jets produced by the hard scattering.

We have already examined this reaction in Sec. 12.14, but without a treatment appropriate for small transverse momentum. Here we write the momenta of the incoming hadron and the detected outgoing hadron as P_A and p_B instead of P and p_h. This notation is consistent with the rest of this chapter, and avoids confusion with use of a subscript h to denote components in the hadron frame. As in Sec. 13.2, we use two coordinate frames: the photon frame and the hadron frame.

The photon frame was used in (12.89), now notated

$$q_\gamma = \left(-x P_{A,\gamma}^+, \ \frac{Q^2}{2x P_{A,\gamma}^+}, \ \mathbf{0}_\text{T} \right), \tag{13.102a}$$

$$P_{A,\gamma} = \left(P_{A,\gamma}^+, \ \frac{M_A^2}{2P_{A,\gamma}^+}, \ \mathbf{0}_\text{T} \right), \tag{13.102b}$$

$$p_{B,\gamma} = \left(\frac{p_{B,\gamma\,\text{T}}^2 + M_B^2}{2p_{B,\gamma}^-}, \ p_{B,\gamma}^-, \ \boldsymbol{p}_{B,\gamma\,\text{T}} \right). \tag{13.102c}$$

Lorentz scalars for the process are x, Q, $z \overset{\text{def}}{=} P_A \cdot p_B / P_A \cdot q$, $|\boldsymbol{p}_{B,\gamma\,\text{T}}|$, and the azimuthal angle $\phi_{B,\gamma}$ of $\boldsymbol{p}_{B,\gamma\,\text{T}}$. Thus $p_{B,\gamma}^- \simeq Q^2 z/(2x P_{A,\gamma}^+)$.

In the hadron frame, both the hadrons have zero transverse momentum:

$$q_h = \left(q_h^+, \ q_h^-, \ \boldsymbol{q}_{h\,\text{T}} \right), \tag{13.103a}$$

$$P_{A,h} = \left(P_{A,h}^+, \ M_A^2/2P_{A,h}^+, \ \mathbf{0}_\text{T} \right), \tag{13.103b}$$

$$p_{B,h} = \left(m_B^2/2p_{B,h}^-, \ p_{B,h}^-, \ \mathbf{0}_\text{T} \right). \tag{13.103c}$$

Since

$$q_{h\,\text{T}}^2 = 2q_h^+ q_h^- + Q^2 \simeq \frac{2p_B \cdot q \ P_A \cdot q}{P_A \cdot p_B} + Q^2, \tag{13.104}$$

we use $\boldsymbol{q}_{h\,\text{T}} = -\boldsymbol{p}_{B,\gamma\,\text{T}}/z$ in the zero-mass limit, and we define the Lorentz transformation between the frames to be

$$\left(V_h^+, \ V_h^-, \ \boldsymbol{V}_{h\,\text{T}} \right) = L \left(V_\gamma^+, \ V_\gamma^-, \ \boldsymbol{V}_{\gamma\,\text{T}} \right)$$

$$= \left(V_\gamma^+ + \frac{2x^2 (P_{A,\gamma}^+)^2 q_{h\,\text{T}}^2 V_\gamma^-}{Q^4} + \frac{2x P_{A,\gamma}^+ \boldsymbol{q}_{h\,\text{T}} \cdot \boldsymbol{V}_{\gamma\,\text{T}}}{Q^2}, \right.$$

$$\left. V_\gamma^-, \ \boldsymbol{V}_{\gamma\,\text{T}} + \boldsymbol{q}_{h\,\text{T}} \frac{2x P_{A,\gamma}^+ V_\gamma^-}{Q^2} \right), \tag{13.105}$$

in an approximation valid *when hadron masses are neglected*. (The formula with hadron masses is more complicated.) Note that the large components of P_A and p_B are unchanged between the frames: $p_{B,h}^- = p_{B,\gamma}^-$ and $P_{A,h}^+ = P_{A,\gamma}^+$ (the last up to a mass-suppressed correction).
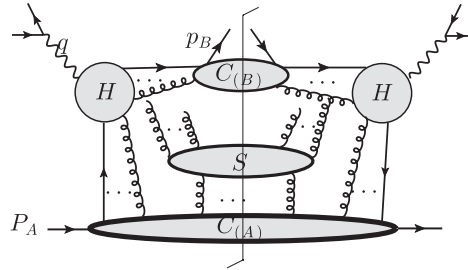
Fig. 13.11. Leading region for SIDIS, for low transverse momentum.

13.15.2 Overall structure of proof

An analysis giving TMD factorization in a CSS-style formalism was first given by Meng, Olness, and Soper (1996), but only when the energy of the outgoing hadron was integrated over. For the unintegrated cross section, a treatment was given by Nadolsky, Stump, and Yuan (2000), and by Ji, Ma, and Yuan (2005). These treatments ignored important quark polarization effects that are absent with integrated parton densities and fragmentation functions. The formalism with polarization effects was provided by Ji, Ma, and Yuan (2004). A list of the necessary structure functions is presented in Kotzinian (1995); Diehl and Sapeta (2005); Bacchetta *et al*. (2007).

Kinematically, SIDIS differs from two-particle-inclusive e^+e^- annihilation simply by crossing one hadron from the final to the initial state, and vice versa for one lepton, thereby making the photon space-like instead of time-like. The graphical specification of the leading regions therefore looks very similar, i.e., Fig. 13.11 for the $q_{h\,T} \ll Q$ case instead of Fig. 13.1.

The same pattern of factorization proof works as for two-particle-inclusive e^+e^- annihilation.

An important change concerns the Glauber region. Previously we simply copied the treatment for the Sudakov form factor, in Sec. 5.5.10. For a Glauber gluon connected to the upper collinear subgraph $C_{(B)}$ in Fig. 13.1, we deformed plus momentum away from final-state poles in $C_{(B)}$, and for a Glauber gluon connected to $C_{(A)}$, we deformed minus momentum away from final-state poles in $C_{(A)}$.

But for SIDIS, there are both initial- and final-state poles in $C_{(A)}$, as in Fig. 12.25. Luckily, as we saw after that figure, it is sufficient to deform away from the final-state poles in $C_{(B)}$, i.e., to make a one-sided deformation.

After the use of region approximators and Ward identities, we get soft and collinear factors whose operators involve Wilson-line factors. Since the deformation to get out of the Glauber region is in the same direction as for e^+e^- annihilation, we can use the same (future-pointing) directions of the Wilson lines, which must not obstruct the contour deformations. Hence the fragmentation function associated with collinear subgraph $C_{(B)}$ is identical to the one in e^+e^- annihilation.

13.15.3 Unpolarized TMD quark density

For the target-collinear subgraph we use a parton density instead of a fragmentation function. Its definition (in transverse coordinate space) is the natural modification of (13.42), again applied in the hadron frame:

$$\tilde{f}_{f/H_A}(x, \boldsymbol{b}_{\mathrm{T}}; \zeta_A; \mu)$$

$$\stackrel{\text{def}}{=} \lim_{\substack{y_A \to +\infty \\ y_B \to -\infty}} \tilde{f}_{f/H_A}^{\text{unsub}}(x, \boldsymbol{b}_{\mathrm{T}}; y_{P_A} - y_B) \sqrt{\frac{\tilde{S}_{(0)}(b_{\mathrm{T}}, y_A, y_n)}{\tilde{S}_{(0)}(b_{\mathrm{T}}, y_A, y_B)\, \tilde{S}_{(0)}(b_{\mathrm{T}}, y_n, y_B)}}$$

$$\times \text{ UV renormalization factor}$$

$$= \tilde{f}_{f/H_A}^{\text{unsub}}(x, \boldsymbol{b}_{\mathrm{T}}; y_{P_A} - (-\infty)) \sqrt{\frac{\tilde{S}_{(0)}(b_{\mathrm{T}}; +\infty, y_n)}{\tilde{S}_{(0)}(b_{\mathrm{T}}; +\infty, -\infty)\, \tilde{S}_{(0)}(b_{\mathrm{T}}; y_n, -\infty)}}$$

$$\times Z_f Z_2. \tag{13.106}$$

The soft factors are exactly the same as for the fragmentation function, but the renormalization factor Z_f may differ. The definition of ζ_A is now

$$\zeta_A \stackrel{\text{def}}{=} 2(k_{A,h}^+)^2 e^{-2y_n} = 2x^2(P_{A,h}^+)^2 e^{-2y_n} = M_A^2 x^2 e^{2(y_{P_A} - y_n)}, \tag{13.107}$$

and the unsubtracted pdf is

$$\tilde{f}_{f/H_A}^{\text{unsub}}(x, \boldsymbol{b}_{\mathrm{T}}; y_{P_A} - y_B) = \mathop{\text{Tr}}_{\text{color}} \int \frac{dw^-}{2\pi} e^{-ixP_A^+ w^-}$$

$$\times \langle P_A | \bar{\psi}_f(w/2) W(w/2; \infty; n_B)^{\dagger} \frac{\gamma^+}{2} W(-w/2; \infty; n_B) \psi_f(-w/2) | P_A \rangle_c$$

$$= \mathop{\text{Tr}}_{\text{color}} \mathop{\text{Tr}}_{\text{Dirac}} \frac{\gamma^+}{2} \int \frac{dk_A^- \, d^{n-2}\boldsymbol{k}_{A\mathrm{T}}}{(2\pi)^n} e^{-i\boldsymbol{k}_{A\mathrm{T}} \cdot \boldsymbol{b}_{\mathrm{T}}} \qquad \tag{13.108}$$
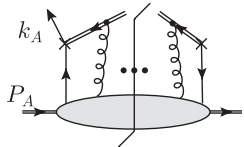
where the vector w in the second line is $(0, w^-, \boldsymbol{b}_{\mathrm{T}})$. The soft factor is defined by (13.39), and the Wilson lines by (13.40). As in Sec. 13.7.2 for fragmentation functions, strictly gauge-invariant operators in the definitions of $S_{(0)}$ and $\tilde{f}^{\text{unsub}}$ would need transverse links to join the Wilson lines at infinity. But, as shown there, their effects cancel in the parton density defined by (13.106).

13.15.4 TMD parton densities: evolution, b_{T} dependence, relation to integrated density

The soft factors in (13.106) are the same as for fragmentation functions. Therefore the CSS evolution equation for the dependence of the TMD quark density on ζ_A is exactly the same

as for TMD quark fragmentation, (13.47), with the same kernel K. Therefore, its anomalous dimension $\gamma_K(g)$ and its non-perturbative part, $g_K(b_T)$ in (13.60), are unchanged.

However, in the RG equation, like (13.50), the anomalous dimension, γ_f, of a TMD quark density may be different, since the quark momentum is reversed.

Because of changed normalizations, the small b_T expansion of the quark density is slightly changed from (13.64):

$$\tilde{f}_{f/H_A}(x, b_T; \zeta_A; \mu) = \sum_j \int_{x-}^{1+} \frac{d\hat{x}}{\hat{x}} \, \tilde{C}_{f/j}(x/\hat{x}, b_T; \zeta_A, \mu, g(\mu)) \, f_{j/H_A}(\hat{x}; \mu) + O\big[(mb_T)^p\big].$$

(13.109)

The coefficient function $\tilde{C}$ need not be the same as for fragmentation.

The analysis of the large-b_T behavior of the TMD density follows as in Sec. 13.11.2. Then the appropriate version of (13.70) giving the separation of perturbative and non-perturbative parts is

$$\tilde{f}_{f/H_A}(x, b_T; \zeta_A; \mu)$$
$$= \sum_j \int_{x-}^{1+} \frac{d\hat{x}}{\hat{x}} \, \tilde{C}_{f/j}\big(x/\hat{x}, b_*; \mu_b^2, \mu_b, g(\mu_b)\big) \, f_{j/H_A}(\hat{x}; \mu_b)$$
$$\times \exp\left[-g_{f/H_A}(x, b_T) - \ln \frac{\sqrt{\zeta_A}}{M_A x} \, g_K(b_T)\right]$$
$$\times \exp\left\{\ln \frac{\sqrt{\zeta_A}}{\mu_b} \tilde{K}(b_*; \mu_b) + \int_{\mu_b}^{\mu} \frac{d\mu'}{\mu'}\left[\gamma_f(g(\mu'); 1) - \ln \frac{\sqrt{\zeta_A}}{\mu'} \gamma_K(g(\mu'))\right]\right\},$$

(13.110)

where $\boldsymbol{b}_*(\boldsymbol{b}_T)$ and μ_b are defined by (13.59) and (13.69). Of the non-perturbative functions, $g_{j/H_A}(x, b_T)$ is specific to parton densities, and cannot be predicted from any measurements of fragmentation functions. But $g_K(b_T)$ is the same as for fragmentation functions.

13.15.5 Hadronic tensor and kinematics of hard scattering

To determine the factorization formula, we follow the same methods as for e^+e^- annihilation. First, we define the hadronic tensor

$$W^{\mu\nu}(q, P_A, p_B) \overset{\text{def}}{=} \sum_X \delta^{(4)}(P_A + q - p_B - p_X)$$
$$\times \langle P_A | j^\mu(0) | p_B, X, \text{out}\rangle \langle p_B, X, \text{out} | j^\nu(0) | P_A\rangle. \qquad (13.111)$$

For each leading region R, an approximator T_R is defined, as in Sec. 13.3.2, generally using hadron-frame coordinates. The only modification is in the approximant for collinear

partons at the hard scattering H, to match the different transformation to the photon frame. Consider unapproximated parton momenta: k_A from the target subgraph to H, and k_B from H to the other collinear subgraph. They have components $k_{A,h} = \left(k_{A,h}^+, k_{A,h}^-, \boldsymbol{k}_{A,h\,T}\right)$ and $k_{B,h} = \left(k_{B,h}^+, k_{B,h}^-, \boldsymbol{k}_{B,h\,T}\right)$. Then we define the approximated momenta by

$$P_{HA}(k_A)_h = \left(k_{A,h}^+, 0, \boldsymbol{0}_\mathrm{T}\right), \tag{13.112a}$$

$$P_{HB}(k_B)_h = k_{B,h}^- \left(\frac{q_{h\,T}^2}{2(q_h^-)^2},\ 1,\ \frac{\boldsymbol{q}_{h\,T}}{q_h^-}\right). \tag{13.112b}$$

From the transformation (13.105), the photon-frame components are

$$P_{HA}(k_A)_\gamma = \left(k_{A,h}^+, 0, \boldsymbol{0}_\mathrm{T}\right), \qquad P_{HB}(k_B)_\gamma = \left(0, k_{B,h}^-, \boldsymbol{0}_\mathrm{T}\right). \tag{13.113}$$

It can be verified that this approximator is unique given the following requirements:

- The total transverse momentum at the hard scattering is unchanged by the approximant. Thus let α and β label the lines between the collinear and hard subgraphs, and let $\hat{k}_{A,\alpha}$ and $\hat{k}_{B,\beta}$ be the approximated momenta. Then from (13.112)

$$\sum_\beta \hat{\boldsymbol{k}}_{B,\beta,h\,T} - \sum_\alpha \hat{\boldsymbol{k}}_{A,\alpha,h\,T} = \sum_\beta \frac{k_{B,\beta,h}^- \boldsymbol{q}_{h\,T}}{q_h^-} = \boldsymbol{q}_{h\,T}, \tag{13.114}$$

where the last equality follows by momentum conservation in the approximated hard scattering.
- The approximated momenta have no transverse components in the photon frame.
- The approximated momenta are massless and on-shell.
- Fractional longitudinal momenta for the partons are the same for the approximated and unapproximated momenta. Thus $\hat{k}_{A,\alpha,h}^+ = k_{A,\alpha,h}^+$ and $\hat{k}_{B,\beta,h}^- = k_{B,\beta,h}^-$.

The first requirement defines what we mean by TMD factorization, while the second and third requirements are how we normally perform a parton-model approximation. The last requirement could be relaxed, but there is no need to; it has the convenience that the longitudinal momentum arguments of the parton densities and fragmentation functions are the standard ones. This follows because the approximated large components of parton momenta obey $\hat{k}_{A,\alpha,\gamma}^+ = k_{A,\alpha,h}^+$ and $\hat{k}_{B,\beta,\gamma}^- = k_{B,\beta,h}^-$. Then momentum conservation, $q = \sum_\alpha \hat{k}_{A,\alpha} + \sum_\beta \hat{k}_{B,\beta}$, in the approximated hard scattering gives

$$\hat{k}_{A,\gamma} = \left(-x P_{A,\gamma}^+, 0, \boldsymbol{0}_\mathrm{T}\right), \qquad \hat{k}_{B,\gamma} = \left(0, \frac{Q^2}{2x P_{A,\gamma}^+}, \boldsymbol{0}_\mathrm{T}\right). \tag{13.115}$$

Hence $\sum_\alpha k_{A,\alpha,h}^+ / P_{A,h}^+ = x$, and $p_{B,h}^- / \sum_\beta k_{B,\beta,h}^- = z$ (up to m^2/Q^2 corrections).

13.15.6 Factorization

The resulting factorization formula is

$$W^{\mu\nu} = \frac{2z}{Q^2} \sum_f \mathrm{Tr} \, \frac{k_{A,\gamma}^+ \gamma^-}{2} \, H_f^\nu(Q; g(\mu), \mu) \, k_{B,\gamma}^- \gamma^+ \, H_f^\mu(Q; g(\mu), \mu)^\dagger$$

$$\times \int \frac{\mathrm{d}^2 \boldsymbol{b}_\mathrm{T}}{(2\pi)^2} e^{-i\boldsymbol{q}_\mathrm{T} \cdot \boldsymbol{b}_\mathrm{T}} \tilde{f}_{f/H_A}(x, \boldsymbol{b}_\mathrm{T}; \zeta_A) \, \tilde{D}_{1, \, H_B/\bar{f}}(z, \boldsymbol{b}_\mathrm{T}; Q^4/\zeta_A)$$

$$+ \text{ polarized terms} + \text{large } q_{h\mathrm{T}} \text{ correction}, Y. \qquad (13.116)$$

Here, the ζ_B argument of the fragmentation function is set to Q^4/ζ_A, corresponding to a similar choice in (13.46). The overall factor $2z/Q^2$ is obtained from the details of the integrals over loop momenta, given the definition of $W^{\mu\nu}$. The hard-scattering factor is the part of the first line of (13.116) after the summation sign. It is normalized to correspond to DIS on an on-shell massless quark in the photon frame. The vertex factor H_f is equipped with soft and collinear subtractions as usual.

13.16 Polarization issues

The explicit TMD factorization term in (13.116) has an unpolarized quark entering the hard scattering, and no sensitivity to the polarization of the quark leaving the hard scattering. The TMD quark density is intended to be defined with an unpolarized initial-state hadron.

There is an interesting set of extensions when one allows for polarization effects. The details get quite complicated, with many structure functions, parton densities and fragmentation functions. A comprehensive list is found in Diehl and Sapeta (2005), but without taking account of the full CSS-style formalism.

The main ideas are quite simple, however. There is a number density of each flavor of parton in a parent hadrons, and the parton has a helicity density matrix. Similarly, the fragmentation function can be sensitive to the polarization state of the outgoing quark (Sec. 13.4.1). In all cases the polarization state of a quark or of a spin-$\frac{1}{2}$ hadron can be described by a three-dimensional Bloch vector (e.g., a helicity λ and a transverse spin $\boldsymbol{S}_\mathrm{T}$), and the spin dependence is linear in the Bloch vector.

The complications arise in enumerating the list of TMD parton densities. In the case of integrated parton densities, rotation and parity invariance restrict the parton densities to an unpolarized density, and helicity and transversity distributions (Sec. 6.5); but with a transverse momentum, the number of possibilities increases substantially.

In the following we let λ and $\boldsymbol{S}_\mathrm{T}$ be the helicity and transverse spin of the target, normalized to maximum values of unity, and we let x and $\boldsymbol{k}_\mathrm{T}$ be the longitudinal momentum fraction and the transverse momentum of the quark. As summarized by Bacchetta *et al.* (2007) and Mulders and Tangerman (1996), we have the following eight densities for a quark in a spin-$\frac{1}{2}$ hadron.

- In an unpolarized hadron:
  - There is a number density of quarks, $f_1(x, k_T)$ in the Mulders-Tangerman notation.
  - The quark can have a transverse polarization proportional to $\epsilon_{ij} k_T^j / M$, where ϵ_{ij} is the two-dimensional antisymmetric tensor. The coefficient $h_1^\perp(x, k_T)$ is called the Boer-Mulders function.
- In a longitudinally polarized hadron with normalized helicity λ:
  - The quark may have a longitudinal polarization proportional to that of the hadron. The coefficient is $g_{1L}(x, k_T)$.
  - The quark may have a transverse polarization proportional to $\lambda k_T / M$. The coefficient is $h_{1L}^\perp(x, k_T)$.
- In a transversely polarized hadron with normalized spin S_T:
  - There may be a contribution to the number density proportional to $\epsilon_{ij} k_T^i S_T^j / M$. The coefficient, $f_{1T}^\perp(x, k_T)$, is called the Sivers function (Sivers, 1990).
  - The quark may have a contribution to its transverse polarization proportional to that of the hadron. The coefficient is $h_1(x, k_T)$.
  - The quark may have a contribution to its transverse polarization proportional to $S_T^j (k_T^j k_T^i - \delta^{ji} k_T^2 / 2) / M^2$. The coefficient, $h_{1T}^\perp(x, k_T)$, is called the pretzelosity distribution.
  - The quark may have a longitudinal polarization proportional to $k_T \cdot S_T / M$. The coefficient is $g_{1T}(x, k_T)$.

The various combinations of pdf and fragmentation contribute to different combinations of structure functions, and contribute to the SIDIS cross section with characteristic angular dependencies listed in Diehl and Sapeta (2005). The longitudinal spin densities are obtained by replacing the trace with γ^+ in (13.108) by a trace with $\gamma^+ \gamma_5$, and the transverse spin densities by replacing γ^+ by $\gamma^+ \gamma^i \gamma_5$.

As for quark fragmentation to an unpolarized hadron, there are (see Sec. 13.4.1) the ordinary number density and the Collins function, which is a final-state analog of the Boer-Mulders function. These allow the cross section to depend on all eight of the TMD densities listed above (Diehl and Sapeta, 2005, Eq. (40)).

See Boer (2009) for the use of the polarized TMD fragmentation functions in $e^+ e^-$ annihilation.

13.17 Implications of time-reversal invariance

Some interesting insights into the nature of QCD factorization and its consequences have resulted from the observation that the Sivers and Boer-Mulders functions have the property called "time-reversal odd", T-odd, for short. As we will see, this means that when we apply a PT transformation we find a reversal of sign. If Wilson lines were ignored in the definitions of these functions, each would be its own negative, and therefore zero. In a gauge theory we do have Wilson lines, and the PT transformation changes them to be past-pointing instead of future-pointing.

As we will see in Ch. 14, parton densities defined with past-pointing Wilson lines are needed for the Drell-Yan process. Thus there is a change of sign between SIDIS and DY (Collins, 2002) for the T-odd functions, i.e., for the Sivers and Boer-Mulders functions.

13.17.1 Sivers function

I now derive (Collins, 1993) the T-odd property of the Sivers function. Rather than a time-reversal transformation, it is convenient to apply a PT transformation, since it leaves momenta of physical states unchanged. It does, however, exchange in-states and out-states, which does not matter for the vacuum and for one-particle states.

Let $\mathcal{PT}$ denote the anti-unitary operator implementing PT transformation on state space. From standard QFT textbooks, we know that the transformation of a quark field is

$$(\mathcal{PT})^{\dagger} \psi(w) \mathcal{PT} = PT \psi(-w), \tag{13.117}$$

where PT is a unitary Dirac matrix such that

$$(PT)^{-1}(\gamma^{\mu})^{*} PT = \gamma^{\mu}. \tag{13.118}$$

There is a possible phase in the transformation (13.117), but it will not affect our proofs. Also from the textbooks, we know that $\mathcal{PT}$ reverses the spin-vector of a single particle state for a spin-$\frac{1}{2}$ particle:

$$\mathcal{PT} |p, S\rangle = \text{phase factor } |p, -S\rangle. \tag{13.119}$$

A bilinear in the quark fields transforms as

$$(\mathcal{PT})^{\dagger} \bar{\psi}(y) \Gamma \psi(z) \mathcal{PT} = \bar{\psi}(-y)(PT)^{\dagger} \Gamma^{*} PT \psi(-z), \tag{13.120}$$

where the $*$ arises because $\mathcal{PT}$ is an antilinear operator. In the case $\Gamma = \gamma^{+}$, as in a quark number density, we get a positive sign: $(PT)^{\dagger}(\gamma^{+})^{*} PT = \gamma^{+}$. For the cases used for spin densities, i.e., $\Gamma = \gamma^{+} \gamma_{5}$ and $\Gamma = \gamma^{+} \gamma_{\mathrm{T}}^{i} \gamma_{5}$, we get a minus sign, which implements the reversal of spin by $\mathcal{PT}$.

Consider now the application of $\mathcal{PT}$ to the operator in a basic parton number density, where we initially work without a Wilson line:

$$\langle P, S| \overline{\psi}_{j}(w/2) \frac{\gamma^{+}}{2} \psi_{j}(-w/2) |P, S\rangle$$

$$= \langle P, S| \mathcal{PT}(\mathcal{PT})^{-1} \overline{\psi}_{j}(w/2) \frac{\gamma^{+}}{2} \psi_{j}(-w/2) \mathcal{PT}(\mathcal{PT})^{-1} |P, S\rangle$$

$$= \langle P, -S| \overline{\psi}_{j}(-w/2) \frac{\gamma^{+}}{2} \psi_{j}(w/2) |P, -S\rangle^{*}$$

$$= \langle P, -S| \overline{\psi}_{j}(w/2) \frac{\gamma^{+}}{2} \psi_{j}(-w/2) |P, -S\rangle. \tag{13.121}$$

The complex conjugate in line 3 arises because of the antilinearity of the $\mathcal{PT}$ operator:

$$\langle f|(\mathcal{PT})^{\dagger}|g\rangle = \langle g|\mathcal{PT}|f\rangle = \langle f'|g\rangle^{*}, \tag{13.122}$$

where $|f'\rangle = \mathcal{PT}|f\rangle$.

Suppose the number density of quarks of some flavor were defined from the matrix element in (13.121), which has no Wilson line. We write the number density in a polarized target as

$$f(x, k_{\mathrm{T}}) + \frac{\epsilon_{ij} k_{\mathrm{T}}^{i} S_{\mathrm{T}}^{j}}{M} f_{1T}^{\perp}(x, k_{\mathrm{T}}), \tag{13.123}$$

where $f_{1T}^{\perp}(x, k_{\mathrm{T}})$ is the Sivers function. From (13.121) it follows the number density is unchanged when the spin vector of the target is reversed, and therefore that the Sivers function vanishes.

This argument is correct in a non-gauge theory. But in QCD (and any other gauge theory), there is a Wilson line going out to infinity in some light-like direction (or approximately light-like direction) from one quark field, and coming back to the other quark field. For the parton densities used for SIDIS, the lines go to *future* infinity. Let us insert this Wilson line in the left-hand side of (13.121). Then the PT transformation to get the right-hand side of (13.121) reverses the positions of the fields, so that on the right-hand side, the Wilson line goes to *past* infinity. We must conclude not that the Sivers function is zero, but that the Sivers function for SIDIS has the opposite sign to a Sivers function with past-pointing Wilson lines.

We will see that, in the Drell-Yan process, proving factorization requires that the TMD parton densities have past-pointing Wilson lines. Thus the Sivers function reverses sign between the two processes:

$$f_{1T,\mathrm{SIDIS}}^{\perp}(x, k_{\mathrm{T}}) = -f_{1T,\mathrm{DY}}^{\perp}(x, k_{\mathrm{T}}), \tag{13.124}$$

while the ordinary unpolarized parton density, $f(x, k_{\mathrm{T}})$, is numerically the same for SIDIS and DY.

The reversal of sign of the Sivers function is a notable violation of the initially intuitive idea that parton densities are universal between processes. In a sense, we already have such violations because of the renormalization-scale dependence of parton densities, and because of the process-dependent directions of Wilson lines in TMD densities.

All of these situations concern controlled and calculable violations of universality: the parton densities (and fragmentation functions) in different reactions and at different energies can be related to each other.

13.17.2 Boer-Mulders function

We generalize (13.121) to measurements of quark polarization by replacing $\gamma^{+}/2$ by the matrix appropriate to a helicity or transversity. In this case, the right-hand side acquires a minus sign. It follows that the Boer-Mulders function is T-odd, since this function is the

transverse spin density of a quark in an unpolarized hadron. The function therefore also reverses sign between SIDIS and Drell-Yan

13.17.3 Other cases

All the other parton densities listed in Sec. 13.16 are T-even. Either they involve no polarization at all, or they involve both a quark polarization and a hadron polarization.

13.17.4 Integrated parton densities

In the definition of integrated densities, the Wilson line goes straight from one quark field to the other, without a detour to infinity. So the Wilson line is unchanged after a PT transformation. So the non-zero integrated parton densities must all be the T-even ones, even in a gauge theory. But this restriction is already implied by rotation and parity invariance, which gave us the simple restriction to a simple number density, a helicity density and a transversity density.

13.17.5 Soft factors and K

The above arguments all apply to the basic operator for a quark density, i.e., to the first factor in definition (13.106). This is multiplied by a particular combination of soft factors. Now the directions of the Wilson lines in the definition (13.39) of the soft factor must match those in the unsubtracted parton density, in order that all the necessary subtractions and the cancellations of rapidity divergences work. So after a PT transformation, the future-pointing Wilson lines in each soft factor S must be replaced by past-pointing Wilson lines.

The value of each S factor is unchanged under this transformation. This is proved by applying the same argument as (13.121) but to the matrix element in (13.39).

Hence the CS and RG evolution equations, including the values of their kernels, are unchanged when the Wilson lines are changed from future to past pointing.

13.17.6 Fragmentation

We have found two types of TMD parton density that are related by a PT transformation and that differ by whether the Wilson lines go to future or past infinity. Naturally, one can ask whether a similar situation arises for fragmentation functions. The answer is in fact negative, as we will now see.

In both the cases treated so far, e^+e^- annihilation and SIDIS, we used future-pointing Wilson lines in the definitions of the fragmentation functions. A PT transformation would indeed convert the Wilson lines to past pointing. But it would also transform out-states to

in-states:

$$\sum_X \text{Tr}\,\gamma^+ \langle 0|\psi(w/2)|p, X, \text{ out}\rangle \langle p, X, \text{ out}|\bar{\psi}(-w/2)|0\rangle$$

$$= \sum_X \text{Tr}\,\gamma^+ \langle 0|\psi(w/2)|p, X, \text{ in}\rangle \langle p, X, \text{ in}|\bar{\psi}(-w/2)|0\rangle . \qquad (13.125)$$

Since in-states with two or more particles are not the same as the out-states with the same labels, but are related by the S matrix, the right-hand side of this equation cannot be equated to a matrix element used to define some fragmentation function.

So PT transformations give no useful information here. Although certain fragmentation functions like the Collins function involve only one spin and are naively T-odd, they can be non-vanishing even in a non-gauge model, unlike the case for a T-odd parton density. To better understand this difference, we insert a complete set of final states between the operators defining a parton density:

$$\sum_X \langle P, S|\,\overline{\psi}_j(w/2)\,|X, \text{ out}\rangle \frac{\gamma^+}{2} \langle X, \text{ out}|\,\psi_j(-w/2)\,|P, S\rangle . \qquad (13.126)$$

Although a PT transformation changes the intermediate states to in-states, we can use completeness in the sum/integral over *all* basis states to convert them back to out-states:

$$\sum_X |X, \text{ in}\rangle \langle X, \text{ in}| = \sum_X |X, \text{ out}\rangle \langle X, \text{ out}| . \qquad (13.127)$$

This argument does not apply to the inclusive sum in a fragmentation function where one particle is detected and therefore not summed over.

Exercises

13.1 Very carefully check all the signs in the derivation and use of the Collins function, notably in (13.31) (13.32), and (13.34).

13.2 (**) Complete problem 10.2 of Ch. 10.

13.3 (***) Find other work on the evolution of TMD parton densities, and try to extend problem 10.2 to it. Such work includes that resulting in the CCFM equation (Ciafaloni, 1988; Catani, Fiorani, and Marchesini, 1990a, b; Marchesini, 1995). Note that the CCFM equation has an apparently radically different structure to the evolution equation described in the present chapter. It nevertheless refers to TMD parton densities, so there should be a relation.

13.4 (**) Find and prove any extensions to the Ward-identity arguments in Ch. 11 that are needed to apply them to the processes treated in this chapter.

13.5 Show that the two-dimensional Fourier transform of an azimuthally symmetric function, defined by (13.35a), can be expressed as a one-dimensional integral:

$$\tilde{S}(b) = 2\pi \int_0^\infty \mathrm{d}k \, k \, J_0(kb) \, S(k), \tag{13.128a}$$

$$S(k) = \frac{1}{2\pi} \int_0^\infty \mathrm{d}b \, b \, J_0(kb) \, \tilde{S}(b), \tag{13.128b}$$

where J_0 is the Bessel function of order zero. This result is used in numerical work.

13.6 (**)
   (a) Generalize the treatment of CSS evolution to include the part of the factorization formula with the Collins function in two-particle-inclusive e^+e^- annihilation.
   (b) Repeat for semi-inclusive DIS, and for the DY process, where the relevant functions also include the Sivers and the Boer-Mulders functions.
   See Idilbi *et al.* (2004) for a solution. You may wish to extend their work.

13.7 (****) Complete the proofs of all the results in this chapter, notably those concerning the application of the subtraction formalism to processes in a non-abelian gauge theory with TMD functions, and the expression of these functions in terms of operator matrix elements with Wilson lines.

13.8 (***) Suppose that, contrary to the argument of Collins and Metz (2004), time-like rather than space-like Wilson lines were used in the definitions of the TMD functions. Determine whether this gives actual problems, and *under what circumstances*. Consider a variety of processes for which TMD functions are appropriate, including two-particle-inclusive e^+e^- annihilation, SIDIS, and DY.
   Notes:
   • Time-like Wilson lines appear to have the advantage of better resembling actual recoil-less partons, at least in e^+e^- annihilation, where the partons have time-like momenta.
   • But in SIDIS and DY each struck parton is space-like, at least as regards its momentum.
   • With time-like Wilson lines, you need to examine very carefully the Collins-Metz arguments about universality.

13.9 (***) If possible, find a simple elegant form for the Feynman rules for computing K beyond lowest order.

13.10 (**) Extend the methods to take account of heavy quarks. Publish the result if you are the first to solve this problem.

13.11 (***) The final definition of the TMD fragmentation function (13.42) involves a product of an unsubtracted fragmentation function and several Wilson-line factors. If possible, express Feynman graphs for this quantity as graphs for the unsubtracted fragmentation function with a systematic subtraction procedure applied. Again, publish the result if you are the first to solve this problem.

13.12 (**) Obtain the coefficients for the small-$b_{\rm T}$ coefficients for the TMD fragmentation functions of gluons; that is, extend the calculations in Sec. 13.14 from quark to gluon fragmentation.

13.13 (***) The formalism presented in this chapter uses TMD fragmentation functions and/or pdfs for the "low-$q_{h\,\rm T}$" terms, and ordinary integrated fragmentation functions and/or pdfs for the large-$q_{h\,\rm T}$ correction. Try to obtain a more unified formalism in which everything is done with TMD functions.